NASA CONTRACTOR REPORT

NASA CR-1162

BUCKLING OF CONICAL SHELLS UNDER AXIAL COMPRESSION

by Johann Arbocz

Prepared by
CALIFORNIA INSTITUTE OF TECHNOLOGY
Pasadena, Calif.
for

NATIONAL AERONAUTICS AND SPACE ADMINISTRATION • WASHINGTON, D. C. • SEPTEMBER 1968

BUCKLING OF CONICAL SHELLS UNDER AXIAL COMPRESSION

By Johann Arbocz

Prepared under Grant No. NsG-18-59 by
CALIFORNIA INSTITUTE OF TECHNOLOGY
Pasadena, Calif.

for

NATIONAL AERONAUTICS AND SPACE ADMINISTRATION

For sale by the Clearinghouse for Federal Scientific and Technical Information
Springfield, Virginia 22151 – CFSTI price $3.00

ACKNOWLEDGMENT

The author wishes to express his sincere appreciation to Dr. E. E. Sechler for his guidance of the work carried out in this investigation. The advice and suggestions of other members of the Department of Aeronautics, especially of Dr. C. D. Babcock is also appreciated.

The help of Miss Helen Burrus for typing and Mrs. Betty Wood with the graphs and figures was very much appreciated.

This study was supported by the National Aeronautics and Space Administration under Research Grant NsG 59-18 and this aid is gratefully acknowledged.

TABLE OF CONTENTS

LIST OF FIGURES

LIST OF FIGURES (Cont'd)

LIST OF TABLES

LIST OF SYMBOLS

E	Young's Modulus
t	Shell thickness
ν	Poisson's ratio
ρ_1	Radius of curvature at the small end of the cone
α	Semivertex angle of the cone
m	Circumferential wave number
h	Height of the truncated cone
R_1	Base radius at the small end

BUCKLING OF CONICAL SHELLS UNDER AXIAL COMPRESSION

By Johann Arbocz
California Institute of Technology

ABSTRACT

An experimental investigation of the effect of the cone semivertex angle α on the buckling load of a conical shell under axial compression was carried out. The effect of a specific type of initial imperfection was also investigated. The imperfection studied was axially symmetric in shape.

The experiments were carried out with shells fabricated by a copper electroforming process. The shells had no longitudinal seams.

Final results showed that the dependence of the buckling load on the semivertex angle α is adequately represented by the linearized theory. Also the upper bound to the experimental results of the cones with known axisymmetric initial imperfections agreed well with previously published analytical values.

INTRODUCTION

The stability of conical shells under axial compression has been studied in the past both theoretically and experimentally by several investigators. Their work showed the same serious disagreement between the experimental data and the results predicted by the small deflection theories of buckling for conical shells as has been encountered previously for cylindrical shells. Among the factors advanced for the explanation of this discrepancy were the extreme sensitivity of the load carrying capacity of shells toward initial imperfections of the order of a fraction of the wall thickness, the nonuniformity of loading around the shell circumference, the influence of boundary conditions, the effect of the prebuckling deformations due to edge constraints and nuclei of plastic strain.

The purpose of the test series reported in this paper was to keep the effect of the above factors and all but one of the shell parameters involved in the stability analysis constant and to investigate the dependence of the buckling load on the remaining free parameter. Thus, in the first part, the dependence of the buckling load on the cone semi-vertex angle α was studied, whereas in the second part the effect on the buckling load of an initial axisymmetric imperfection of known shape was investigated.

FABRICATION OF THE TEST SPECIMENS

The conical shells used for this testing program were fabricated by electroforming on wax mandrels. This process was used previously for the fabrication of cylindrical shells (Ref. 1).

About an inch thick layer of wax was first cast on water cooled mandrels having the proper cone angle. The wax used was a two to one mixture of refined paraffin and Mobile Cerese Wax 2305. This wax was used because it had been shown by previous work with cylindrical shells that it could be cast free of air bubbles and that it had the proper machining characteristics. After the wax had hardened it was machined to the shape of the shell desired. A pivot type lathe tracer attachment made by the True Trace Corporation was used on a standard lathe to machine both the initially perfect conical mandrels and the conical mandrels with an initial axisymmetric imperfection. After the desired form was obtained the wax was spray painted with a silver paint thinned with Tolune. Since the plate at the top of the mandrel was used to carry the electrical current to the surface of the wax form, the paint had to cover this plate.

The plating was carried out in a Copper Fluoborate bath. Because of the previous experience with electroforming cylindrical shells, copper was retained as the plating material. Also it has been shown that of all the materials suited for this type of experimental work, copper has the lowest internal stresses developed during the plating process (Ref. 1). Control of the plating process consisted of a PH measurement with calorimetric paper to control the acid content and a

density measurement to control the copper concentration. During the plating, the bath was agitated both by the rotating cathode and by forced air. The anodes were bagged with a Dynel fabric to collect the anode sludge that would otherwise accumulate in the tank. Also the plating solution was continuously filtered during the plating process. Occasionally the bath was treated with activated charcoal to remove organic impurities that could cause a rough brittle plate if not removed. A standard transformer rectifier and powerstat was used to give a uniformly varied current up to 130 amps. At full power the current density was about 55 amps per square foot. The plating time was approximately 20 minutes per 0.001 inches of plate. The plating was carried out at room temperature. The conical mandrels were rotated during the plating so as to assure circumferential uniformity of plating of the finished shell. Figure 2 shows the plating installation.

After the plating was completed, the mandrel was rinsed thoroughly and the shell cut to the desired length while it was still on the mandrel. In order to keep the large end radius constant extreme care had to be observed for proper placement of these cuts. This was accomplished by referring the initial cut to a premachined surface on the upper plate of the mandrel. After the cutting operation the shells were then removed from the mandrel by melting out the wax. This was accomplished by pouring hot wax over the shell so as to melt a thin layer of wax directly under the surface. Then the mandrel was immersed in a bath of hot wax. The excess wax and silver paint was removed from the finished shells with benzene. Figure 1 shows a completed test shell.

A. Wall Thickness

When switching from cylindrical to conical shells considerable difficulty was encountered in trying to obtain a uniform thickness distribution along the generator of the conical shells. It was found that the plate tended to build up to a greater thickness towards the ends of the mandrel. This was especially severe for cones with semivertex angle $\alpha = 20^{\circ}$ and $\alpha = 25^{\circ}$. This problem has been solved by placing the anodes properly inclined in the plating bath. By this method the thickness

variation was kept to $\pm$ 5 per cent of its nominal value. This compares very favorably with the values published in reference 2 where thickness variations up to $\pm$ 15 per cent of the nominal values were reported.

The average thickness of the test shells was determined before the buckling test by weighing the shells. The specific gravity used in the calculation of thickness was 8.9.

The thickness variation along the generator of the cones was checked initially by cutting strips out of the first test specimens and determining their thickness by an optical comparator. Table I and Fig. 3 through 5 show some typical measurements of thickness distribution.

B. Material Properties

Initially it was found that the plated copper had a very low yield point. This was quite undesirable from the buckling part of the experiment, especially at higher semivertex angles where the stresses close to the smaller end would exceed the yield strength of the material before elastic buckling could occur. It was found that the adding of about 10 cc of New Orleans black strap molasses per gallon of plating solution would not only raise the modulus of elasticity of the plated copper from 13.10^6 psi to about $15.5.10^6$ psi but at the same time the yield strength of the plated copper would also improve considerably.

Tests to determine the characteristic of the plated copper were carried out in uniaxial tension. This was done by utilizing long strips of the plated copper which were soldered into 1/8 inch thick plates that were in turn clamped into the jaws of an Instron testing machine. The strips were cut from the upper straight portion of the conical mandrels. The strips had length to width ratios of about 80. The head displacement of the testing machine was used as the measure of strain and the load read from the Instron load cell. A typical stress-strain curve is shown in Fig. 6. The results of the tests are shown in Table II.

A determination of Poisson's ratio for each shell was not attempted since its influence in the reduction of the buckling data is of secondary importance. A value of 0.3 was used for this purpose.

TEST PROCEDURE

To carry out the buckling tests of conical shells a controlled end-displacement type testing machine was designed (see Fig. 7). By the use of matched pairs of high precision thrust bearings the axial elastic displacement under load of the testing machine was kept to a minimum thus making the testing machine rigid in comparison with the test specimen. The relative displacement of the two end plates of the testing machine was controlled by four loading screws, which could be adjusted independently to give the proper load distribution on the shell, or simultaneously to increase the load up to the critical value. One complete turn of the screws gave a displacement of 0.025 inches. Figure 8 shows the details of these displacement controlling screws. The springs shown in Fig. 7 were used to preload the testing machine when installing the test specimen in the machine and securing it to the upper end plate of the testing machine. The testing was carried out when the machine was in the position shown in Fig. 7. The end plate with the gear drive rested on pins and the opposite end rested on a set of rollers. By this arrangement the frictional torque produced when turning the gears was transmitted through the pins into the base plate on which the testing machine rested, and the test specimen was loaded by axial compression only.

During the buckling tests the load distribution was monitored and the total load was obtained by means of the load cell shown in Fig. 9. It consisted of a seamless, electroformed copper cylinder which was 0.015 inches thick, 3.00 inches long and 8.000 inches in diameter. Twenty-four foil type strain gages were mounted on the cylinder equally spaced around the circumference. The ones on the inside were directly opposite to those on the outside. The difficulty of adequate end support for the cones with different semivertex angles was solved by providing the upper ring on the load cell, which acts as a mount for the test specimen, with a removable insert. Thus all the cones with different semivertex angle could be installed into the same load cell by simply using the proper insert. However, in order to support the upper end of

the conical shells, a different end ring was used for every cone semi-vertex angle. The load cell was secured to the end-plate of the testing machine with a thin layer of Devcon. Devcon is a plastic-like material in a putty state which hardens in several hours after the addition of a hardening agent. Finally the test shell was cast with the low melting point alloy Cerrolow into an end ring and its other end was secured to the load cell in the same manner. After this operation was completed the end ring was secured to the upper end plate by a thin layer of Devcon. Upon hardening of the Devcon the cone was ready for testing. Figure 10 shows the complete conical shell testing configuration. It has been shown in reference 1 that the strain measured by this type of arrangement represented very accurately the actual strain in the test shell.

Before carrying out the buckling tests the gages on the load-cell were connected to a 24 channel bridge box which contained 24 Wheatstone bridge circuits. In order to minimize the effect of temperature changes an additional 24 strain gages were installed on a dummy cylinder and connected to the same bridge box where they formed one of the branches of the individual Wheatstone bridge circuits. The initial zero reading could be adjusted individually through differential shunt balances. The output of the bridge was monitored by a Cimron Digital Voltmeter. By using the Data Control Unit connected between the bridge and the digital voltmeter the readings of the 24 strain gages were recorded automatically by means of an IBM card punch. The total compressive load in the load cell was computed by averaging the readings of all gages and using a previously determined calibration factor. The calibration of the load-cell was carried out using a very accurate Schaevitz dynamometer-type load ring.

A. Buckling Procedure

The buckling tests were carried out in the following manner. The conical shells were initially loaded to about one-sixth of the expected buckling load and the circumferential load distribution was made as uniform as possible by individually adjusting the four loading screws of

the testing machine. The load was then increased in small increments by turning the four loading screws simultaneously. After each increase the load distribution was adjusted again. This was carried out up to about two-thirds of the expected buckling load. After this point the load distribution was no longer adjusted so as to prevent buckling occurring during one of the adjustments. The load was increased in small increments and the strain gages monitored until buckling occurred.

B. Initial Imperfection Measurements

In the test series of imperfect conical shells the same form of axisymmetric initial imperfection was machined into the conical mandrels by using the same template with the pivot type lathe tracer attachment. The imperfection measurements on the cones already installed in the testing machine were made with a reluctance type non-contacting pick-up consisting of an iron core through which passed a 100.000 Hz signal. The impedance of the coil to this signal changes as the electromagnetic field of the coil is disturbed by the eddy currents generated in an external conducting surface. By determining the change in impedance of the coil the position of the external surface relative to the end of the pick-up could be measured quite accurately. The pick-up signal was read on a Cimron digital voltmeter. The output of the pick-up was about 1.00 volt per 0.001 inch with a working range of approximately 0.150 inches. The noise level and drift were minimized so that a deflection of 10^{-4} inches could be accurately read without making contact with the measured surface.

The measurements were carried out by mounting the sensing head of the pick-up in a slide which traveled on an adjustable guide. The guide was carefully lapped to insure that it was as straight as possible. Figure 11 shows the pick-up and the guide. The guide was attached to the testing machine, its inclination adjusted so as to be parallel to the surface of the cone to be measured and readings were taken at 25 stations along the generator. Thus in this series of tests the initial imperfection that was measured was the deviation of the generator of the shell from a straight line. Figure 12 shows the initial imperfection measuring equipment in position on a cone.

TEST RESULTS - "perfect" Conical Shells

Previously reported experimental investigations (Ref. 2) showed that when compared with the results predicted by the linearized, small deflection theories of buckling the experimental values were much lower and the data had a large scatter band. In the past decade the following five factors found acceptance as an explanation of the discrepancy between theory and experiments:

1. Initial geometrical imperfections of the order of a fraction of the wall thickness.
2. Nonuniformity of load distribution around the shell circumference.
3. Influence of boundary conditions.
4. Effect of prebuckling deformation caused by edge constraints.
5. Nuclei of plastic strain.

As noted in the introduction the purpose of these test series was to keep the effect of the above factors and all but one of the shell parameters constant thus studying the dependence of the buckling load on the remaining free parameter. By using electroformed copper shells not only was the size of the initial imperfections minimized but also seamless test specimens of great uniformity were obtained. Wall thickness was constant to within $\pm$ 5 per cent and variations in the cone geometry were less than 1 per cent. Also, by being able to adjust the four loading screws individually, variation in the load distribution around the circumference of the shell was kept to $\pm$ 7 per cent. Since all the cones were cast into end rings with Cerrolow, and buckled following exactly the same test procedure, hence we can expect equal influence from items (3), (4), and (5) on the final collapse load of each individual shell.

For these tests the base radius R_1, the height of the truncated conical shells h and their wall thickness t were kept constant, while the semivertex angle α of the cones was varied from 0 through 25°. Detailed results of the buckling tests for perfect conical shells are summarized in Table III. The buckling results for all those shells that

had visible localized initial buckling were excluded from this list because there is every reason to believe that all local bucklings were caused by some pronounced localized defect in the test specimen. These defects could have been caused during the removal of the shell from the wax mandrel or by the subsequent handling required for the installation of the same in the testing machine. This local buckling consisted of the formation of one or more waves on the surface of the shell causing the load distribution to fall off in the neighborhood of these waves without appreciably affecting the distribution over the rest of the circumference of the shell. After the initial local buckling, the load was increased until general collapse occurred without attempting to adjust the load distribution. General collapse occurred in the same manner as for the cones that did not have an initial local buckling, but at lower values of axial loading.

General collapse consisted of a snap-through which is characteristic of this type of test. For all cases the postbuckling state consisted of 2 to 3 rows of buckles that extended completely around the circumference. The number of circumferential waves is noted in Table III. Closer to the smaller end seemed to be the preferred place for the buckling to take place.

As stated in the previous section, the load distribution was adjusted to be as uniform as possible with the four loading screws of the testing machine. The adjustment was done by equalizing the strain in the load cell at the 45°, 135°, 225°, and 315° positions. This adjustment was not attempted after about 75 per cent of the expected buckling load was obtained. Table III gives the maximum variation in load distribution near buckling. The average maximum variation in load distribution for all the shells tested was 13.9 per cent. Figure 13 through 17 show typical load distributions as measured on the load cell. Several distributions are given on these figures as the load on the shell was increased. Figures 18 through 22 give the load distribution on the shells at the last reading before buckling. It should be remarked here that strain gage N° 6 of the load cell turned out to be faulty which may explain the consistently higher readings at the 150° position.

The final results are summarized in Figs. 23 and 24 which show the variations of $P/P_{c\ell}$ with cone semivertex angle α and with the ρ_1/t ratio respectively. Both figures indicate that all of the shells tested have a relatively small scatter band, most of the experimental points lying between 0.6 - 0.7. Also the lower bound of these experimental values is considerably higher than those reported by other investigators. For the sake of comparison, Fig. 25 shows a similar plot reproduced from reference 2, where the lower bound was about 0.33.

The reason for the high values of buckling load is not completely understood, however they could be explained by the following items:

1. All of the cones had no seams. The effect of the seam on the buckling load is an uninvestigated effect. In the tests carried out in the past, it was usually assumed that if the buckling did not appear to initiate at the seam, and the seam did not interfere with the postbuckling state then the seam had no effect. The validity of this assumption is not known.

2. All of the cones had a thickness variation of $\pm$ 5 per cent only as compared to test specimens in reference 2 which had thickness variations of up to $\pm$ 15 per cent.

3. Variations in the circumferential load distribution were kept to 13.9 per cent. The influence of load distribution is actually also an unknown factor. Very little data has been published on this aspect of buckling tests. The data that has been published by Babcock (Ref. 1), by Lo, Crate and Schwartz (Ref. 3) show a maximum variation of about 19 per cent.

4. All the cones tested were very sensitive to how their edges were built into the end rings. For satisfactory results the spacers had to be fitted individually to every cone. If they were too tight or too loose buckling would occur at very low values of axial loading.

5. Finally there is the effect of unwanted initial imperfections. By the electroforming process and by extremely careful handling of the finished test specimen it was possible to minimize the size of the unintended initial imperfections. No actual measurements were carried out to determine their size so no comparison can be made with conical shells tested in axial compression by other investigators.

TEST RESULTS - "imperfect" Conical Shells

As mentioned earlier, the fact that the load carrying capacity of cylinders was extremely sensitive to initial imperfections has found acceptance as an explanation of the discrepancy between theory and experiment. Recent work by several investigators (Refs. 2 and 4) have shown that there exists the same discrepancy between theoretical and experimental values when considering conical shells under axial compression.

Thus motivated by the analytical results published by Schiffner (Ref. 4), a test series was carried out to investigate the effect of an axially symmetric imperfection on the buckling load under axial compression. Figure 26 shows the intended imperfection of the conical shells. It was taken directly from reference 4. Figures 27 through 29 show the measured imperfections of these shells after they had been installed in the testing machine.

Detailed results of the buckling tests for imperfect conical shells are summarized in Table IV. General collapse consisted of a snap-through. In all cases where the cone semivertex angle α was less than 20° the postbuckling state consisted of one row of buckles that extended completely around the circumference. The number of circumferential waves is noted in Table IV. In all cases the buckling took place at the central portion of the cone where the initial imperfection was located. For the cones with semivertex angle $\alpha = 20^{\circ}$ and $\alpha = 25^{\circ}$ the post-buckling state consisted of two distinct rows of buckles that extended completely around the circumference, the additional row occurring towards the larger end. It should also be noted here that localized initial buckling was encountered with only one of the imperfect conical shells tested. This can be explained by the fact that in the other cases the degrading effect of the intended axially symmetric imperfections was greater than the degrading effect of certain localized defects that might have been present in the test specimen.

The final results are summarized in Figs. 30 and 31 which show the variations of $P/P_{c\ell}$ with cone semivertex angle α and with the ρ_1/t ratio respectively. Once again both figures indicate that all of the shells tested have a relatively small scatter band, most of the experi-

mental points lying between 0.35 - 0.4. The upper bound of these experimental values is at 0.45.

CONCLUSION

The results plotted in Fig. 23 confirmed the prediction of several investigators (Refs. 4 and 5) who claimed that for $\alpha < 45^{\circ}$ the effect of the cone semivertex angle α on the buckling load is adequately represented by the result of the linearized theory where

$$P_{c\ell} = C \frac{2\pi Et^2}{\sqrt{3(1-\nu^2)}} \cos^2 \alpha$$

The constant C accounts for the decrease in the theoretical buckling load due to the prebuckling deformation caused by the edge constraints. It was shown in reference 4 and 5 that C is essentially independent of the cone semivertex angle α for simply supported and built in boundary conditions. Comparing the lower bound to the buckling loads from Fig. 24 of 0.6 with the analytical result of Kobayashi (Ref. 5) of 0.92, who solved the stability problem of a conical shell under axial compression including the effects of built-in edge conditions and the effect of the prebuckling deformation on the buckling load, we are still left with a discrepancy of 0.32. However, as has been shown by Schiffner (Ref. 4), one can easily account for even this decrease in buckling load if we include in the anlysis the effects of initial imperfections. For the sake of mathematical simplicity he chose the axisymmetric imperfection shown in Fig. 26.

The results of a series of tests on conical shells with the same axisymmetric imperfection plotted in Figs. 30 and 31 confirmed qualitatively the analytical predictions. The upper bound of these experimental values is at 0.45 which agrees very well with the results published by Schiffner (Ref. 4).

REFERENCES

1. Babcock, C. D.: The Buckling of Cylindrical Shells with an Initial Imperfection under Axial Compression Loading. Ph. D. Thesis, California Institute of Technology, 1962.
2. Weingarten, V. I.; Morgan, E. T.; and Seide, P.: Final Report on Development of Design Criteria for Elastic Stability of Thin Shell Structures. STL/TR-60-000-19425, Space Technology Laboratories, 1960.
3. Lo, Hsu; Crate, M.; and Schwartz, E. B.: Buckling of Thin Walled Cylinder under Axial Compression and Internal Pressure. NACA Report 1027, 1951.
4. Schiffner, K.: Spannungs-und Stabilitatsuntersuchungen an Dunnwandigen Kegelschalen Bei Axialsymmetrischen Randbedingungen. DLR FB 66-24, 1966.
5. Kobayashi, Shigeo: Influence of Prebuckling Deformation on the Buckling Load of Truncated Conical Shells under Axial Compression, NASA CR 707, 1967.

TABLE I

THICKNESS DISTRIBUTION ALONG THE

GENERATOR OF THE CONES

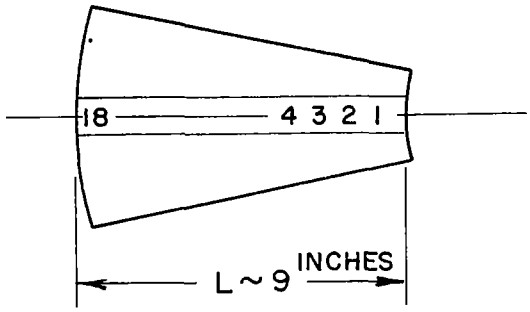

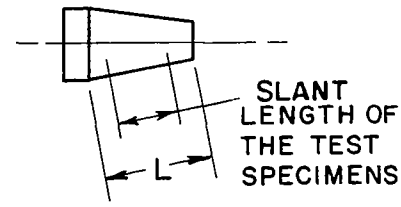

Thickness Measured At The Positions On The Shell Surface Indicated Above

Thickness Inches x 10^3

Position	Shell N^ox 4 $\alpha = 5^o$	Shell N^ox 3 $\alpha = 10^o$	Shell N^ox 5 $\alpha = 15^o$	Shell N^ox 11 $\alpha = 20^o$	Shell N^ox 15 $\alpha = 25^o$
1	3. 54	3. 46	4. 00	4. 93	5. 46
2	3. 64	3. 32	3. 87	4. 82	5. 04
3	3. 58	3. 29	3. 83	4. 71	4. 75
4	3. 55	3. 29	3. 83	4. 74	4. 61
5	3. 46	3. 27	3. 82	4. 72	4. 50
6	3. 37	3. 24	3. 84	4. 65	4. 51
7	3. 33	3. 35	3. 82	4. 75	4. 53
8	3. 28	3. 22	3. 78	4. 71	4. 50
9	3. 31	3. 21	3. 86	4. 69	4. 51
10	3. 33	3. 21	3. 88	4. 62	4. 51
11	3. 31	3. 22	3. 95	4. 65	4. 45
12	3. 32	3. 21	3. 93	4. 60	4. 50

TABLE I (Cont'd)

THICKNESS DISTRIBUTION ALONG THE

GENERATOR OF THE CONES

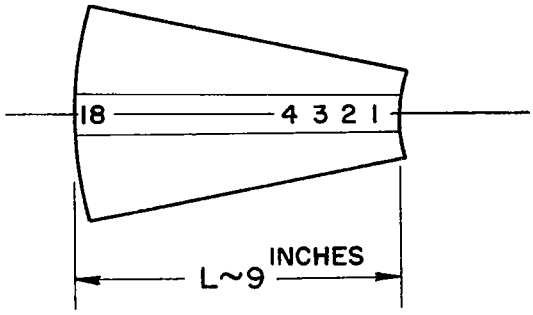

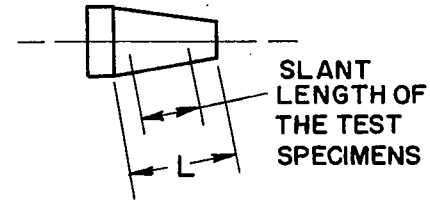

Thickness Measured At The Positions On The Shell Surface Indicated Above

Thickness Inches x 10^3

Position	Shell N^ox 4 $\alpha = 5^o$	Shell N^ox 3 $\alpha = 10^o$	Shell N^ox 5 $\alpha = 15^o$	Shell N^ox 11 $\alpha = 20^o$	Shell N^ox 15 $\alpha = 25^o$
13	3.34	3.21	4.04	4.60	4.48
14	3.37	3.20	4.05	4.60	4.45
15	3.36	3.19	4.05	4.70	4.49
16	3.43	3.22	4.05	4.94	4.57
17	3.44	3.22	4.04	5.10	4.78
18	3.20	3.23	4.06	5.50	5.38

TABLE II

YOUNG'S MODULUS TESTS

FOR PLATED COPPER

Shell	α Degrees	$t \times 10^3$ inches	Plating Date	E Lbs/in^2
5A5	5	4.18	8-15-67	13.6
5A6	5	3.31	8-21-67	13.3
5A7	5	3.77	8-28-67	13.0
10A1	10	4.50	3-15-67	14.4
10A3	10	3.79	7-12-67	14.5
10A6	10	3.93	9-15-67	14.3
15A1	15	3.96	8-14-67	13.4
15A3	15	3.82	8-28-67	13.0
15A6	15	3.85	9-20-67	14.3
20A1	20	4.08	9-15-67	14.9
20A2	20	4.00	9-19-67	14.5
20A4	20	3.99	9-25-67	14.9
25A1	25	3.95	7-31-67	14.0
25A10	25	3.60	10-11-67	15.4
25A11	25	3.69	10-17-67	16.4

TABLE II (Cont'd)

YOUNG'S MODULUS TESTS

FOR PLATED COPPER

Shell	α Degrees	$t \times 10^3$ inches	Plating Date	E Lbs/in^2
5I1	5	3.67	9-25-67	14.5
5I2	5	3.88	10-18-67	15.5
5I3	5	3.88	11-25-67	14.8
10I1	10	3.92	10- 4-67	15.3
10I2	10	3.79	11-29-67	14.5
10I3	10	3.90	12- 5-67	15.1
15I1	15	3.90	9-27-67	14.5
15I2	15	3.91	10-19-67	14.5
15I3	15	3.85	11-14-67	15.0
20I1	20	3.76	12-19-67	15.4
20I2	20	3.94	1- 5-68	14.6
20I3	20	4.03	1-10-68	15.3
25I1	25	3.84	11-15-67	15.7
25I2	25	3.89	11-21-67	15.0
25I3	25	3.81	12-27-67	15.0

Remarks:

Without adding the proper amount of Black Strap Molasses Young's modulus of the plated copper is about 13.0×10^6. Several times during the test series the plating solution had to be treated by activated charcoal, which accounts partially for the scatter of the Young's moduli of shells plated on different days.

TABLE III

SUMMARY OF BUCKLING TESTS

ON "PERFECT" CONICAL SHELLS

Shell	α	$t \times 10^3$	ρ_1	$\frac{\rho_1}{t}$	$\frac{P}{P_{c\ell}}$	$\frac{\sigma_{max} - \sigma_{min}}{\sigma_{Ave}}$ %	m	Remarks
	Degrees	Inches	Inches					
5A5	5	4.18	3.693	884	0.59	18.5	15-16	Snap buckling on the central portion of the cone
5A6	5	3.31	3.693	1115	0.66	9.8	17	Snap buckling close to the smaller end
5A7	5	3.77	3.693	979	0.63	10.7	15	Snap buckling close to the smaller end
10A1	10	4.50	3.014	670	0.70	15.0		Snap buckling close to the smaller end
10A3	10	3.79	3.014	795	0.80	4.6		Snap buckling close to the smaller end
10A6	10	3.93	3.014	767	0.61	10.9		Snap buckling close to the smaller end
15A1	15	3.96	2.314	585	0.64	17.0		Snap buckling on the central portion of the cone
15A3	15	3.82	2.314	606	0.67	12.8	16-17	Snap buckling on the central portion of the cone
15A6	15	3.85	2.314	601	0.65	19.9	16	Snap buckling close to the larger end

TABLE III (Cont'd)

SUMMARY OF BUCKLING TESTS

ON "PERFECT" CONICAL SHELLS

Shell	α	$t \times 10^3$	ρ_l	$\frac{\rho_l}{t}$	$\frac{P}{P_{c\ell}}$	$\frac{\sigma_{max} - \sigma_{min}}{\sigma_{Ave}}$ %	m	Remarks
	Degrees	Inches	Inches					
20A1	20	4.08	1.561	383	0.67	14.4	16	Snap buckling close to the smaller end
20A2	20	4.00	1.561	390	0.72	14.6	16	Snap buckling close to the smaller end
20A4	20	3.99	1.561	391	0.64	14.0	15	Snap buckling close to the smaller end
25A1	25	3.95	0.715	181	0.65	7.7	12	Snap buckling close to the smaller end
25A10	25	3.60	0.715	199	0.65	20.0	13	Snap buckling close to the larger end
25A11	25	3.69	0.715	194	0.63	18.0	13	Snap buckling on the central portion of the cone

All shells had a height of 8.000 inches.

TABLE IV

SUMMARY OF BUCKLING TESTS

ON "IMPERFECT" CONICAL SHELLS

Shell	α	$t \times 10^3$	ρ_1	$\frac{\rho_1}{t}$	$\frac{P}{P_{c\ell}}$	$\frac{\sigma_{max} - \sigma_{min}}{\sigma_{Ave}}$ %	m	Remarks
	Degrees	Inches	Inches					
5I1	5	3.67	3.693	1006	0.40	6.9	14	One row of buckles
5I2	5	3.88	3.693	952	0.35	7.2	13	One row of buckles
5I3	5	3.88	3.693	952	0.38	10.7	13	One row of buckles
10I1	10	3.92	3.014	769	0.39	18.6	13	One row of buckles
10I2	10	3.79	3.014	795	0.39	11.2	14	One row of buckles
10I3	10	3.90	3.014	773	0.38	5.6	12	One row of buckles
15I1	15	3.90	2.314	593	0.36	10.8	11	One row of buckles
15I2	15	3.91	2.314	592	0.40	7.3	11	One row of buckles
15I3	15	3.85	2.314	601	0.33	43.5	12	Local buckling over 1/3 of the circumference

TABLE IV (Cont'd)

SUMMARY OF BUCKLING TESTS

ON "IMPERFECT" CONICAL SHELLS

Shell	α Degrees	$t \times 10^3$ Inches	ρ_1 Inches	$\frac{\rho_1}{t}$	$\frac{P}{P_{c\ell}}$	$\frac{\sigma_{max} - \sigma_{min}}{\sigma_{Ave}}$ %	m	Remarks
20I1	20	3.76	1.561	415	0.44	8.1	12	One and a half rows of buckles
20I2	20	3.94	1.561	396	0.44	17.4	11	One row of buckles
20I3	20	4.03	1.561	387	0.42	16.0	12	One row of buckles
25I1	25	3.84	0.715	186	0.42	7.2	12 -13	Two rows of buckles
25I2	25	3.89	0.715	184	0.42	14.2	12 -12	Two rows of buckles
25I3	25	3.81	0.715	188	0.45	12.2	12 -13	Two rows of buckles

FIG. 1 COMPLETED TEST SPECIMEN

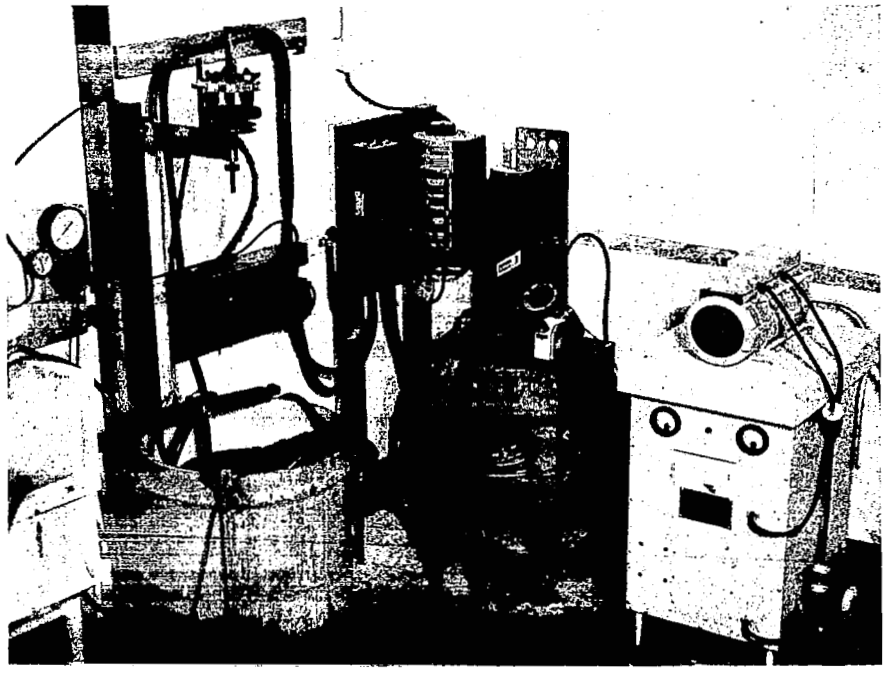

FIG. 2 PLATING INSTALLATION

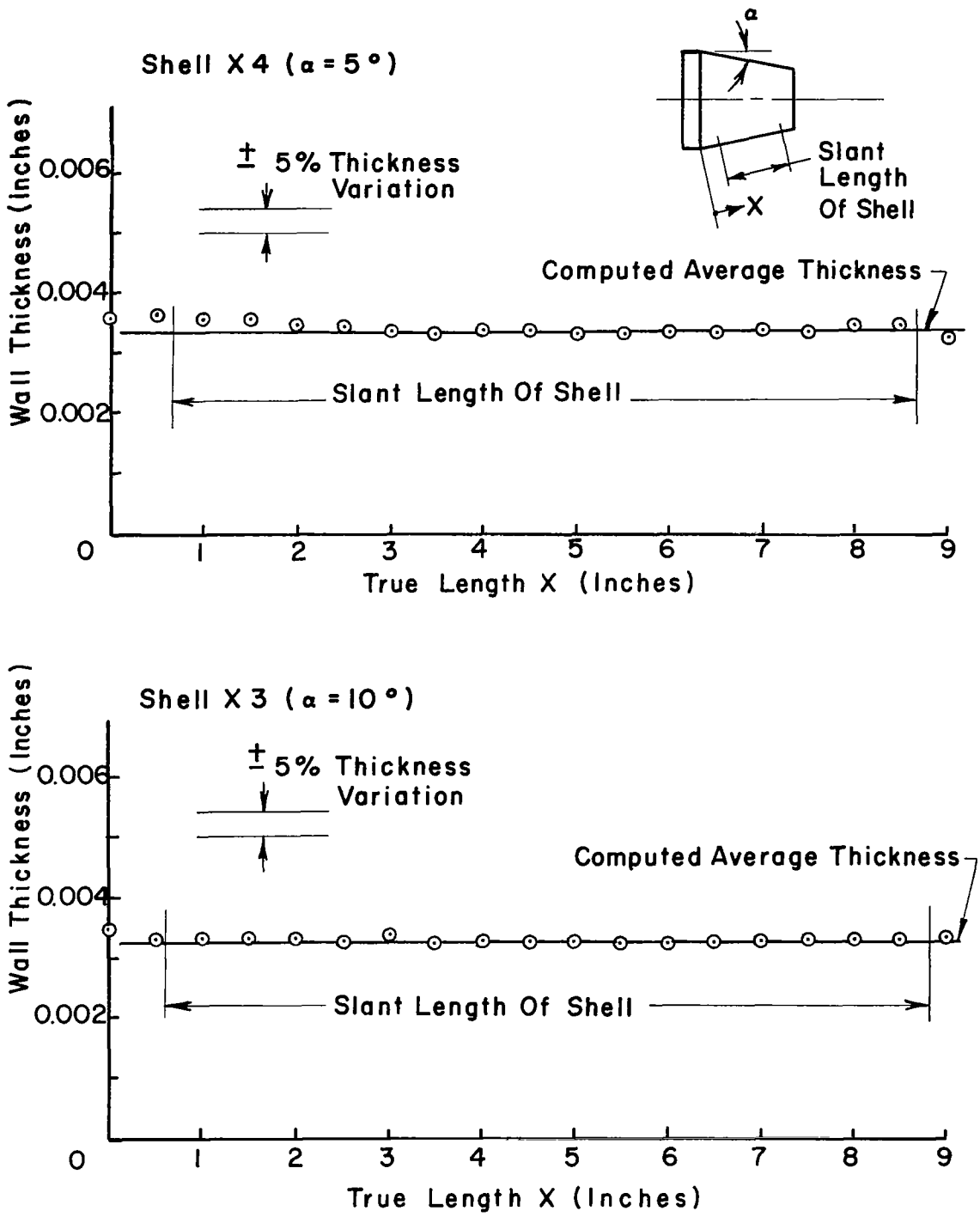

FIG. 3 THICKNESS DISTRIBUTION ALONG THE GENERATOR OF CONICAL SHELLS

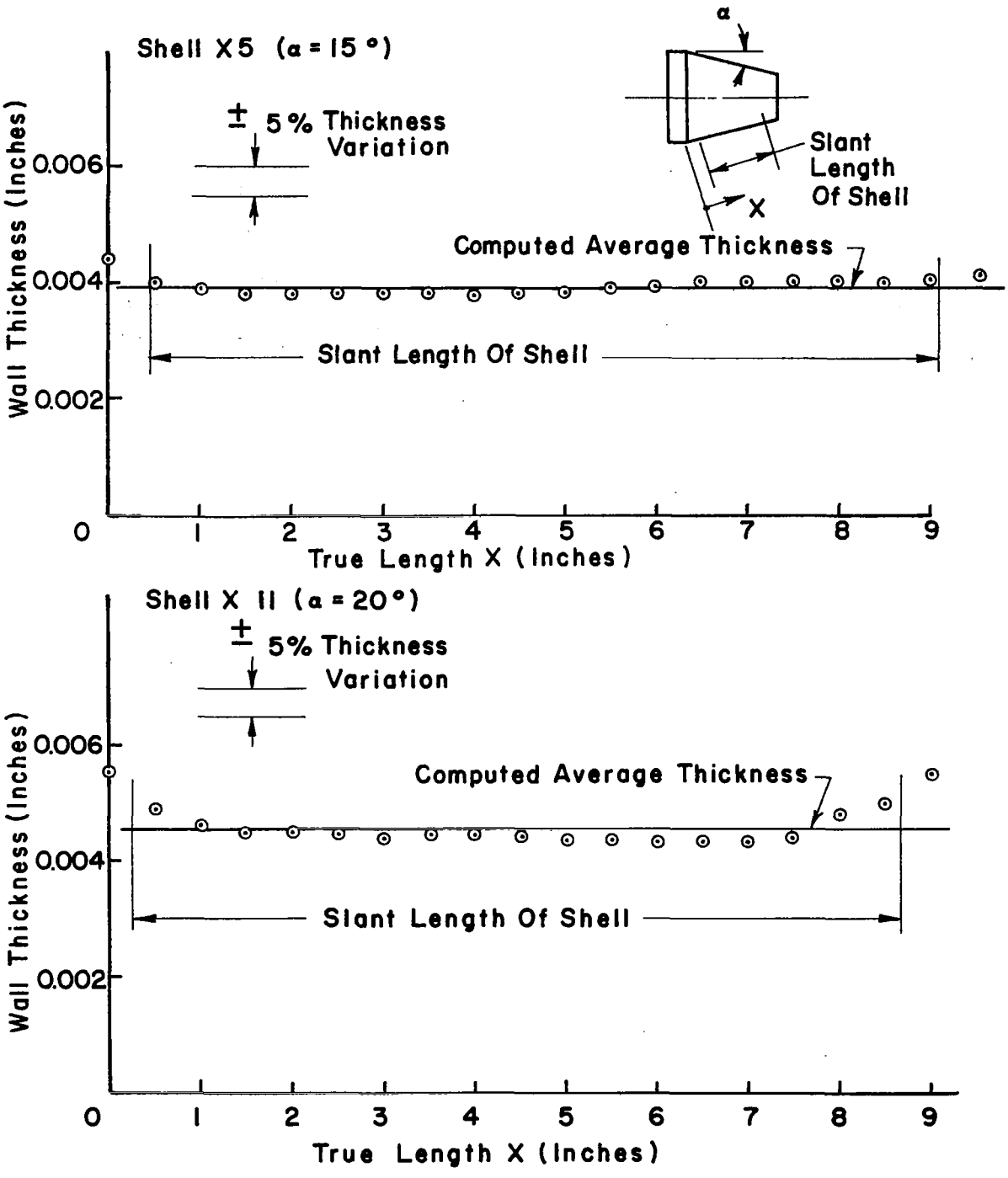

FIG. 4 THICKNESS DISTRIBUTION ALONG THE GENERATOR OF CONICAL SHELLS

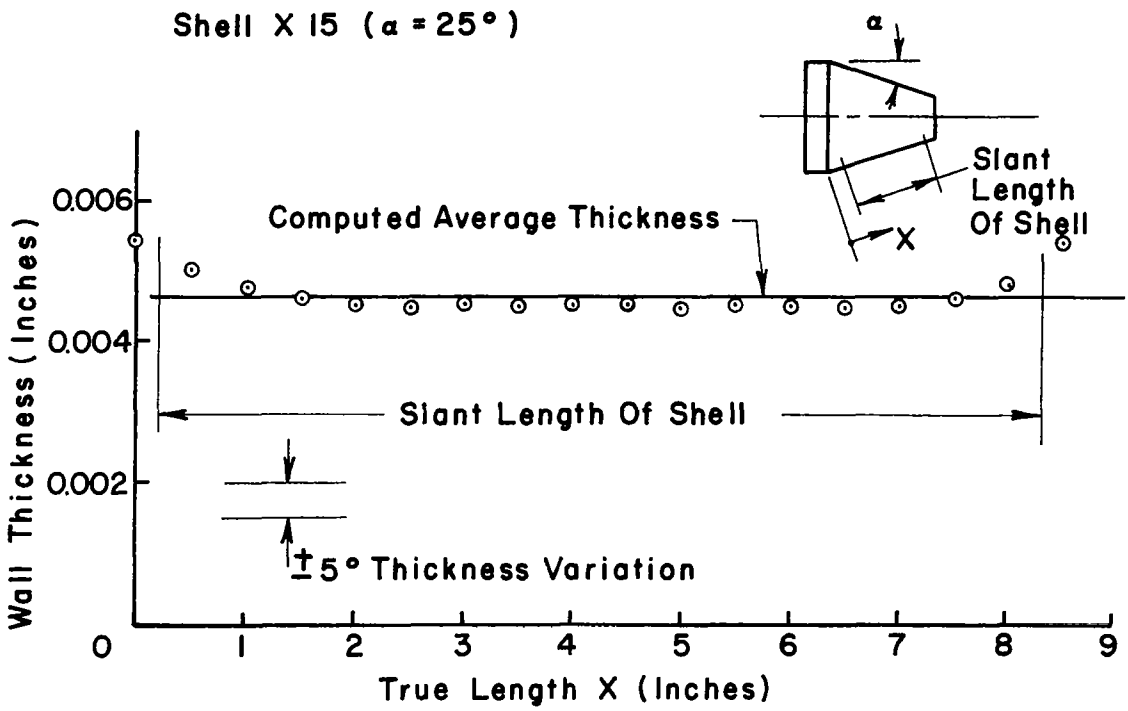

FIG. 5 THICKNESS DISTRIBUTION ALONG THE GENERATOR OF CONICAL SHELLS

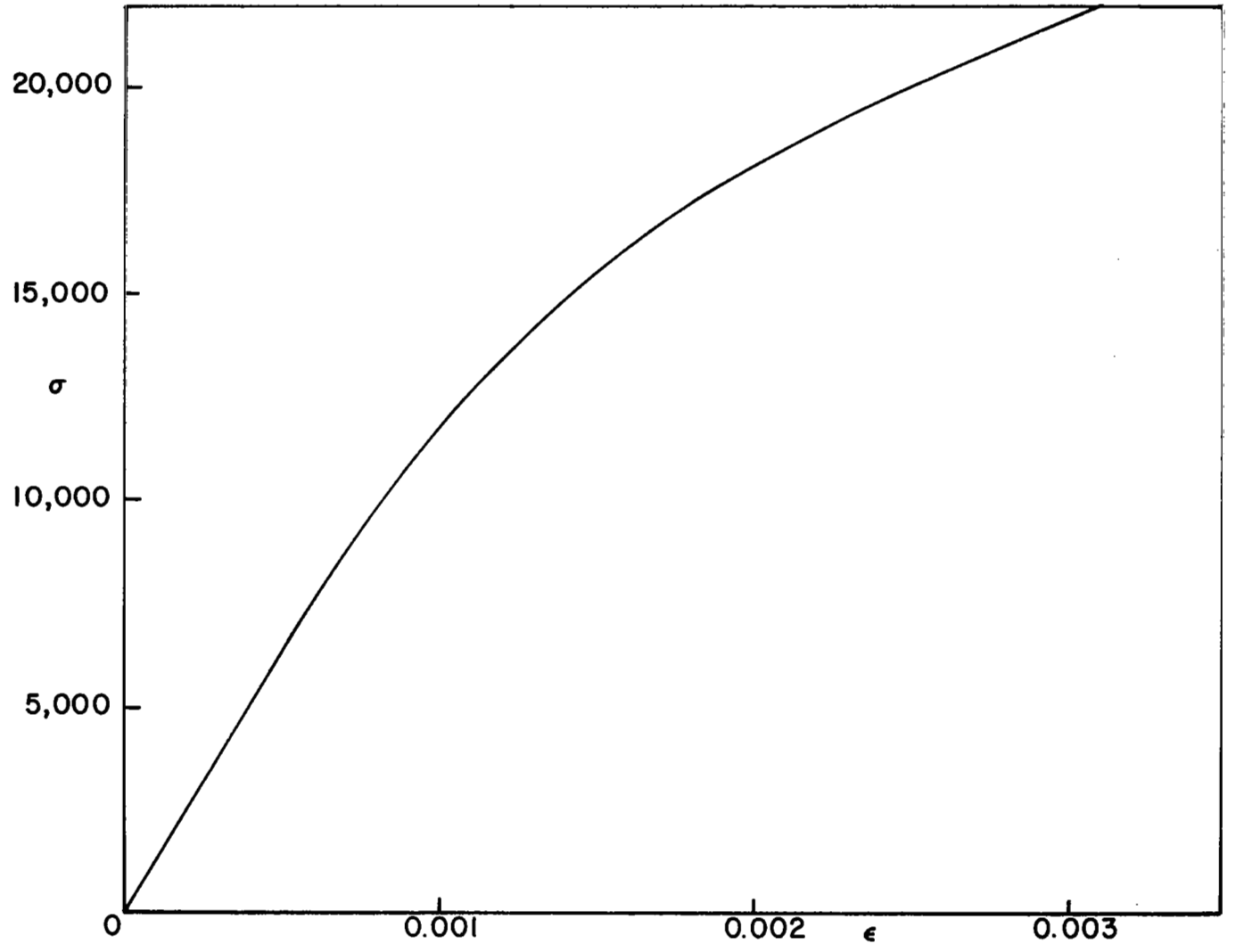

FIG. 6 STRESS STRAIN CURVE FOR PLATED COPPER

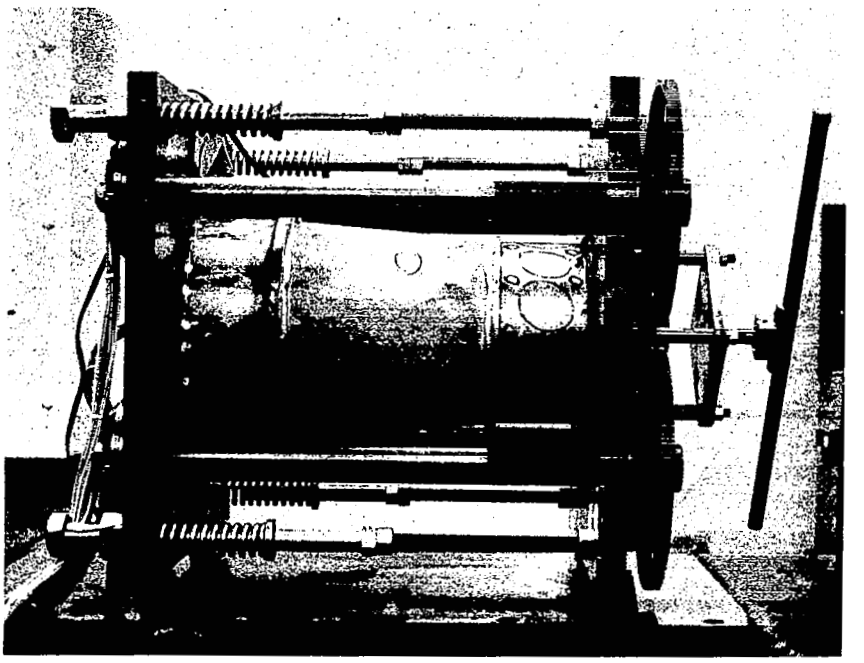

FIG. 7 TESTING MACHINE

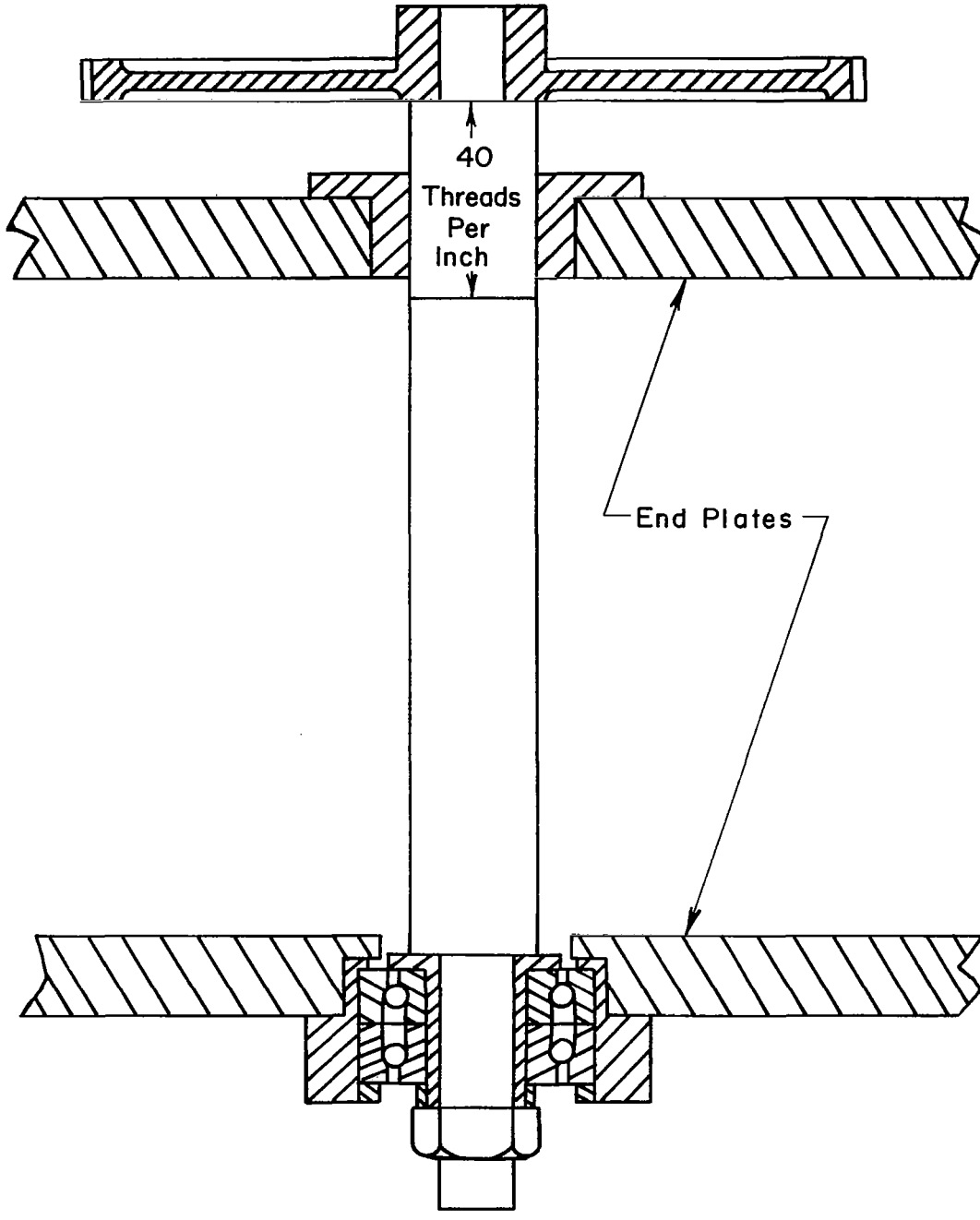

FIG. 8 DETAILS OF TESTING MACHINE LOADING SCREW

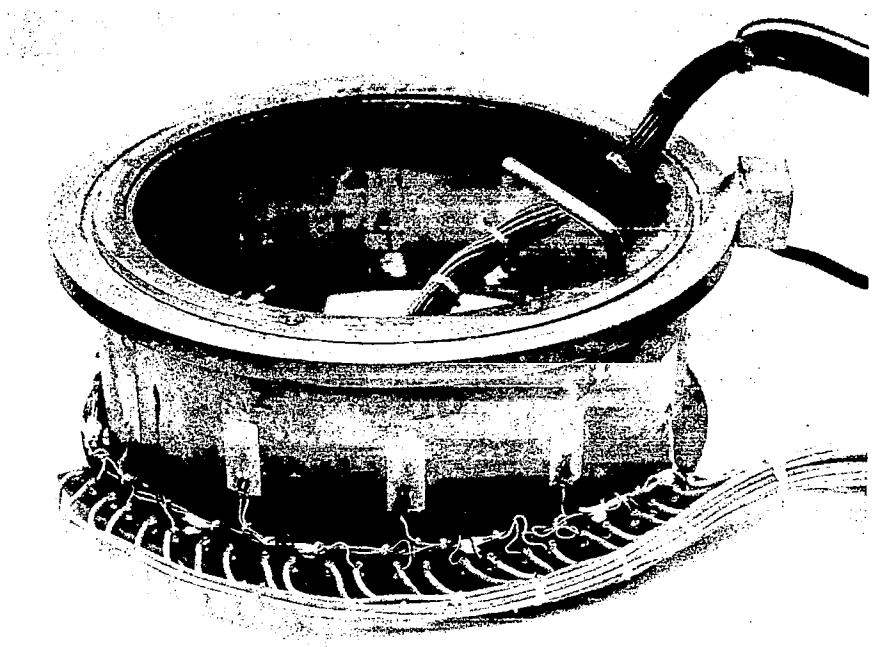

FIG. 9 LOAD CELL

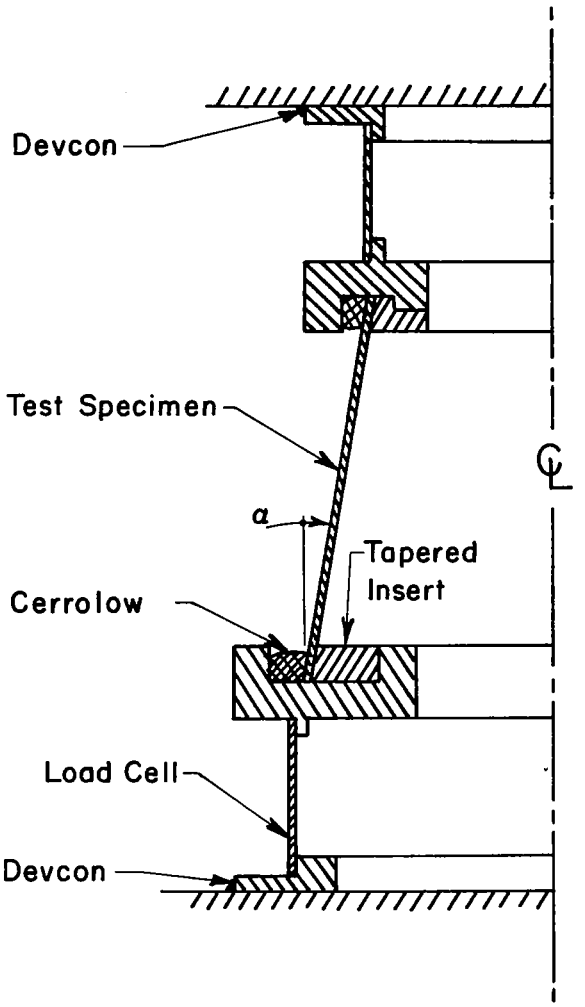

FIG. IO CONICAL SHELL TESTING CONFIGURATION

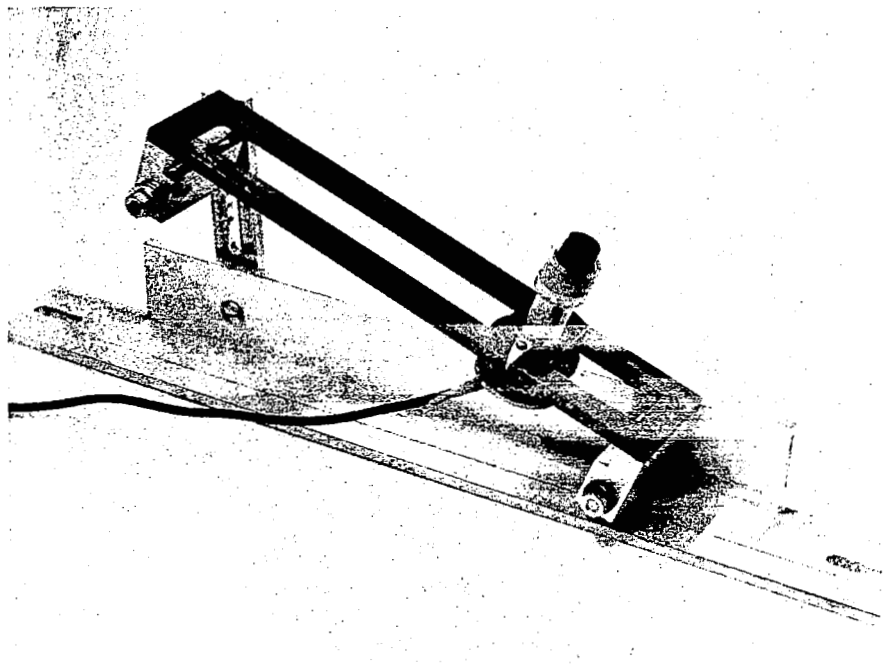

FIG. 11 INITIAL IMPERFECTION MEASURING EQUIPMENT

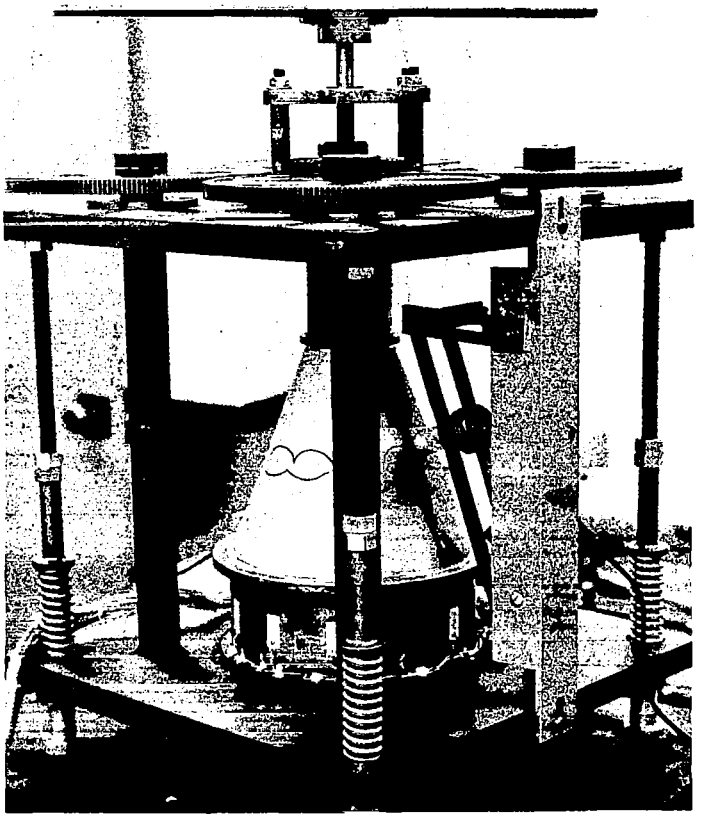

FIG. 12 INITIAL IMPERFECTION MEASURING EQUIPMENT IN POSITION ON A CONE

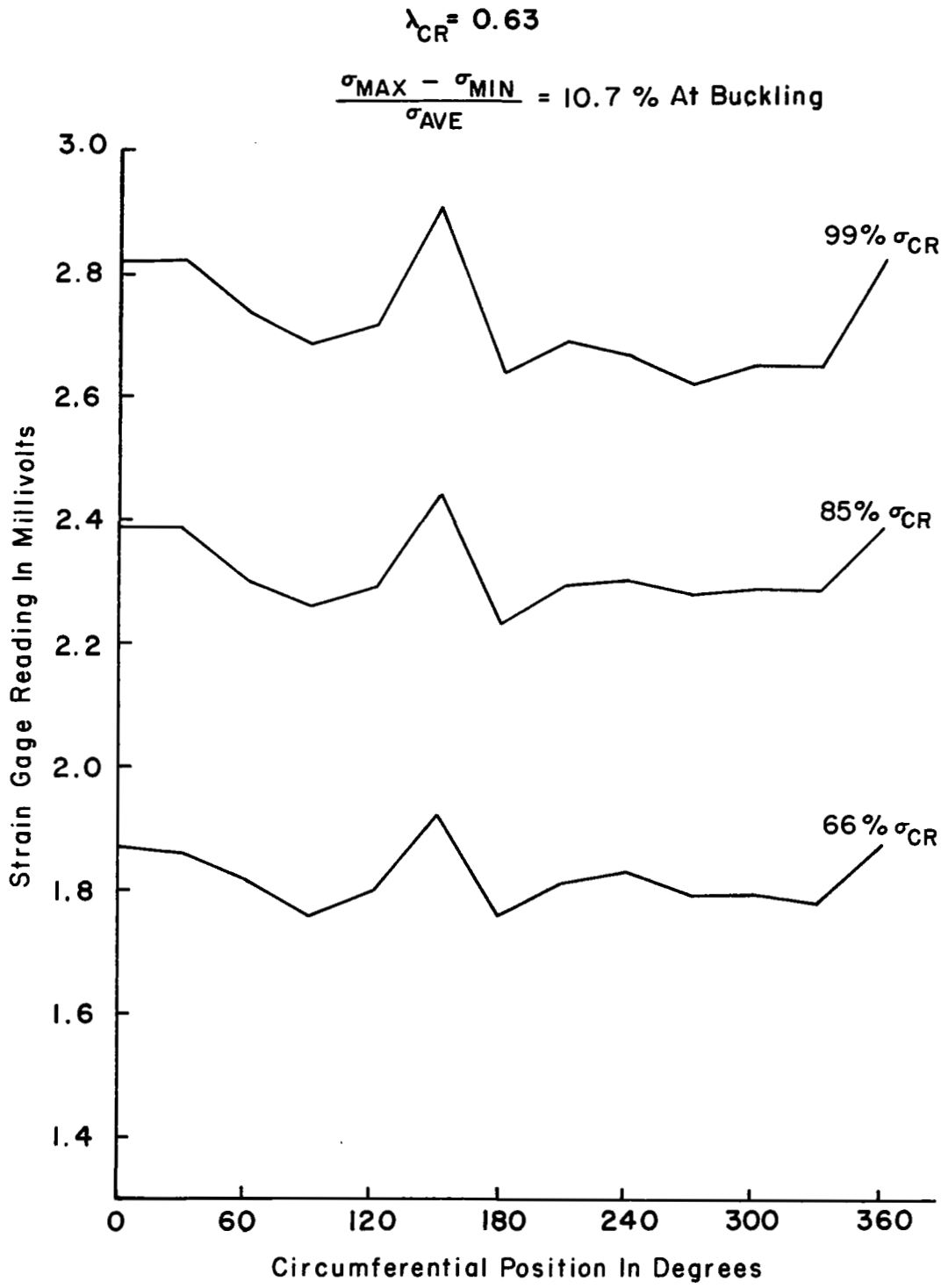

FIG. 13 SHELL 5A7 LOAD DISTRIBUTION

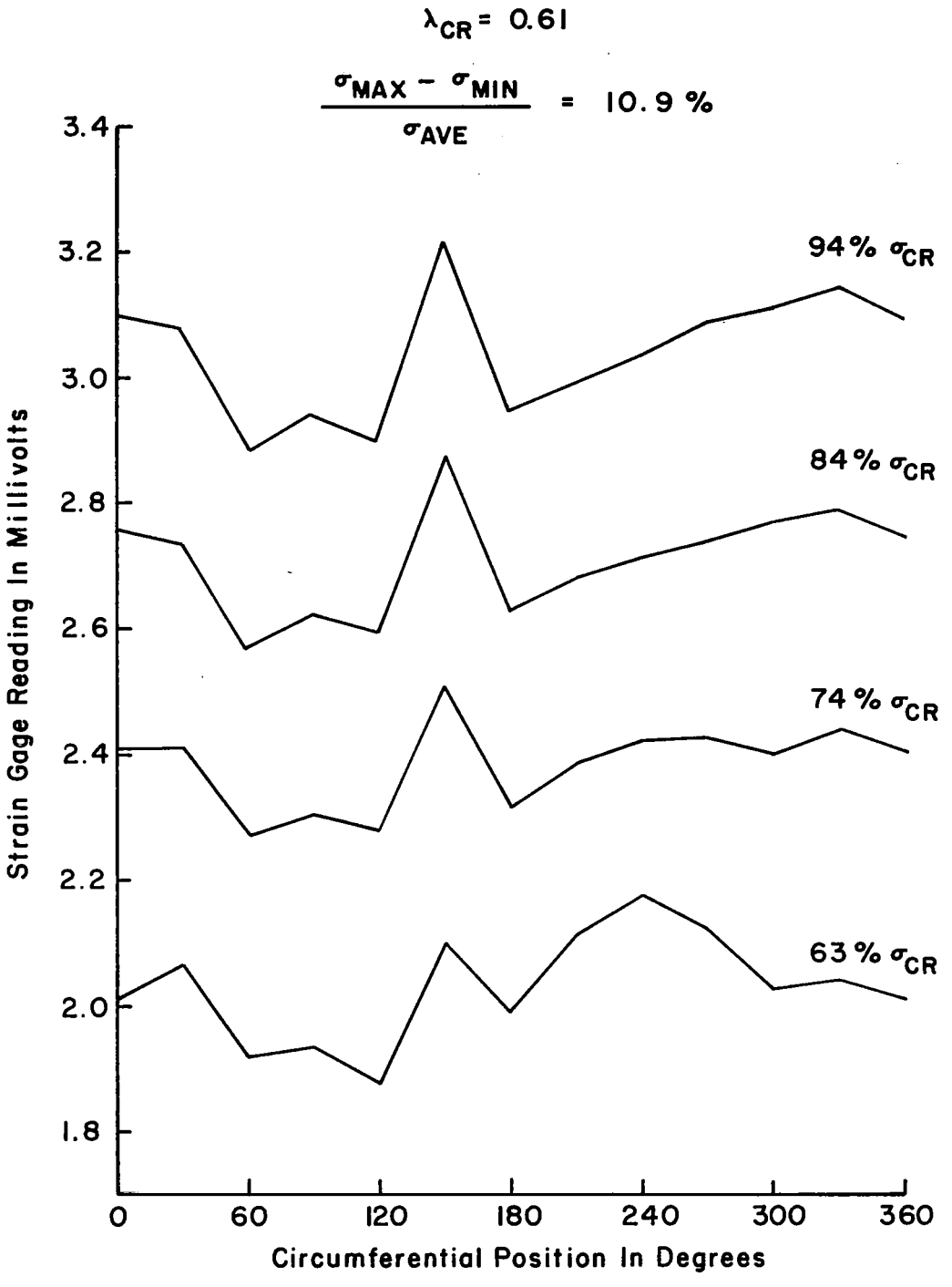

FIG. 14 SHELL 10A6 LOAD DISTRIBUTION

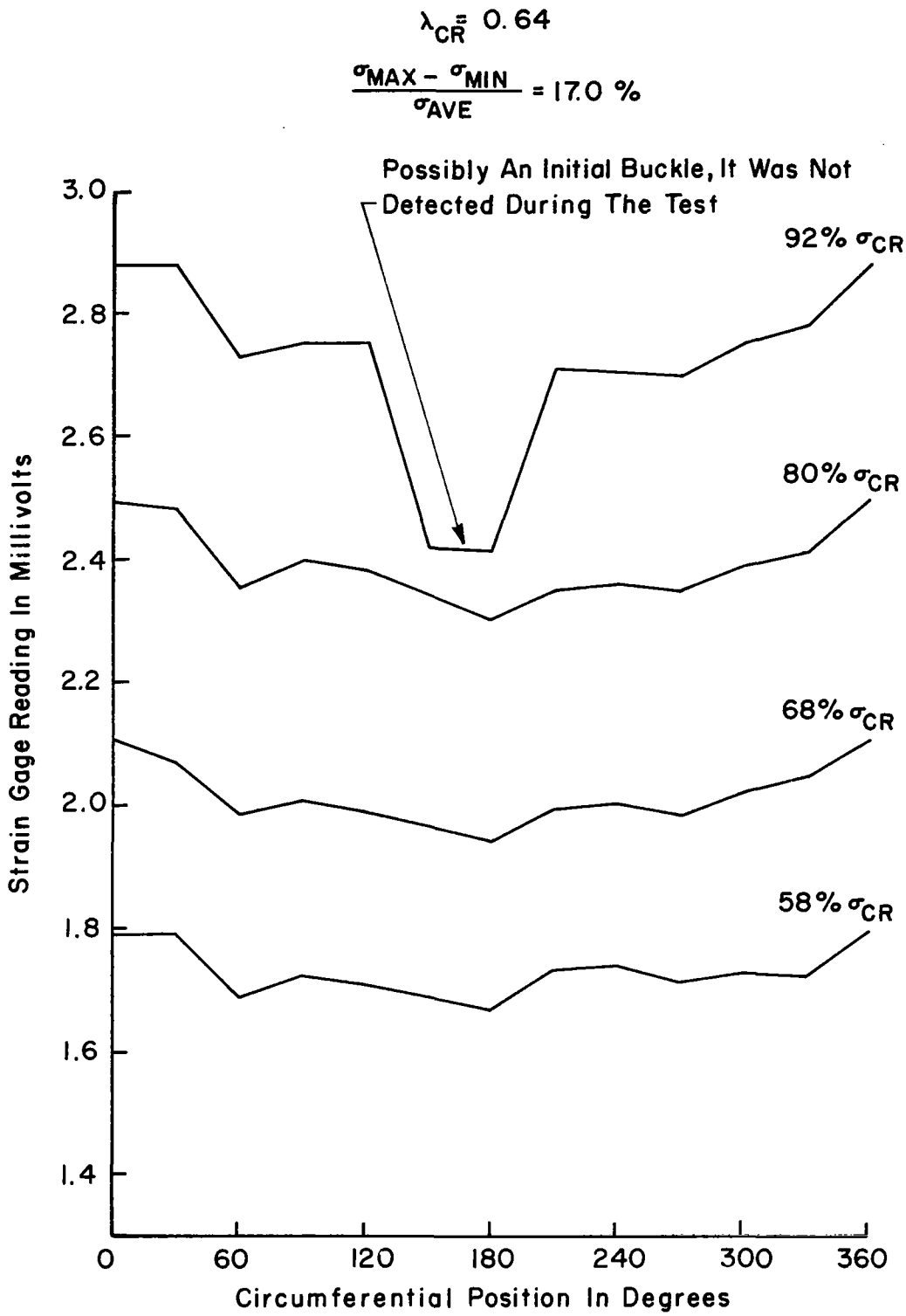

FIG. 15 SHELL 15 AI LOAD DISTRIBUTION

$\lambda_{CR} = 0.64$

$$\frac{\sigma_{MAX} - \sigma_{MIN}}{\sigma_{AVE}} = 14.0\%$$

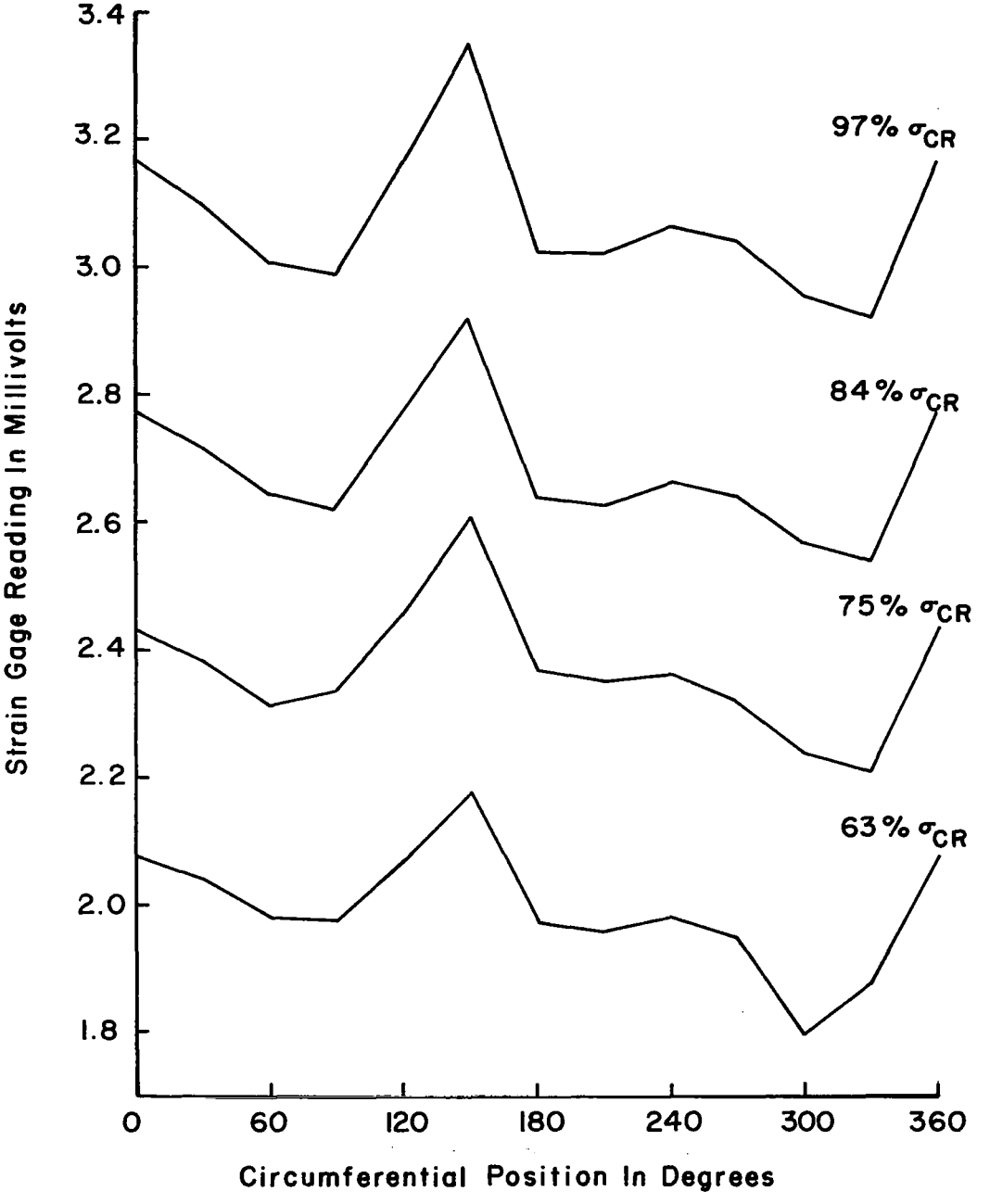

FIG. 16 SHELL 20A 4 LOAD DISTRIBUTION

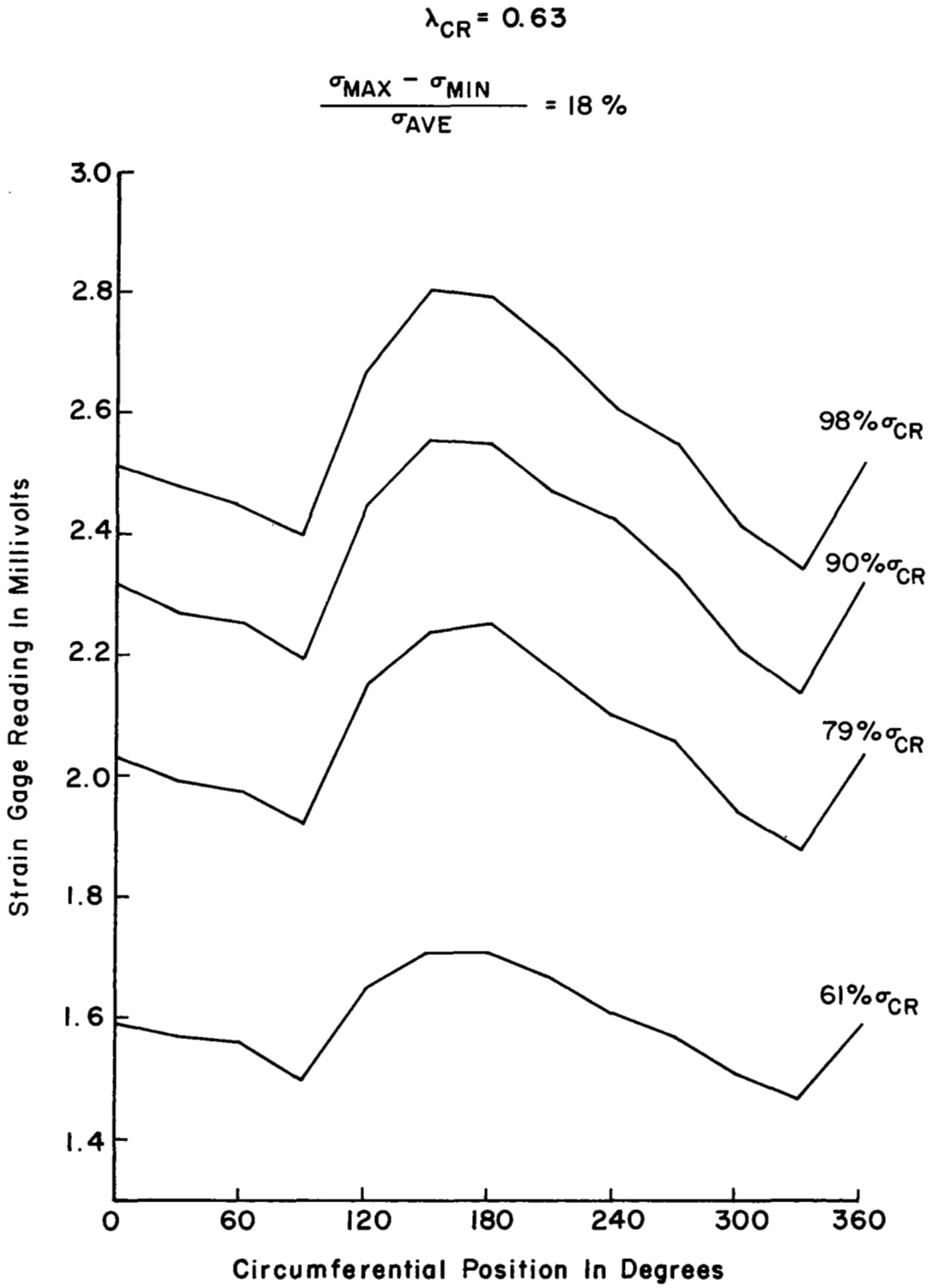

FIG. 17 SHELL 25A 11 LOAD DISTRIBUTION

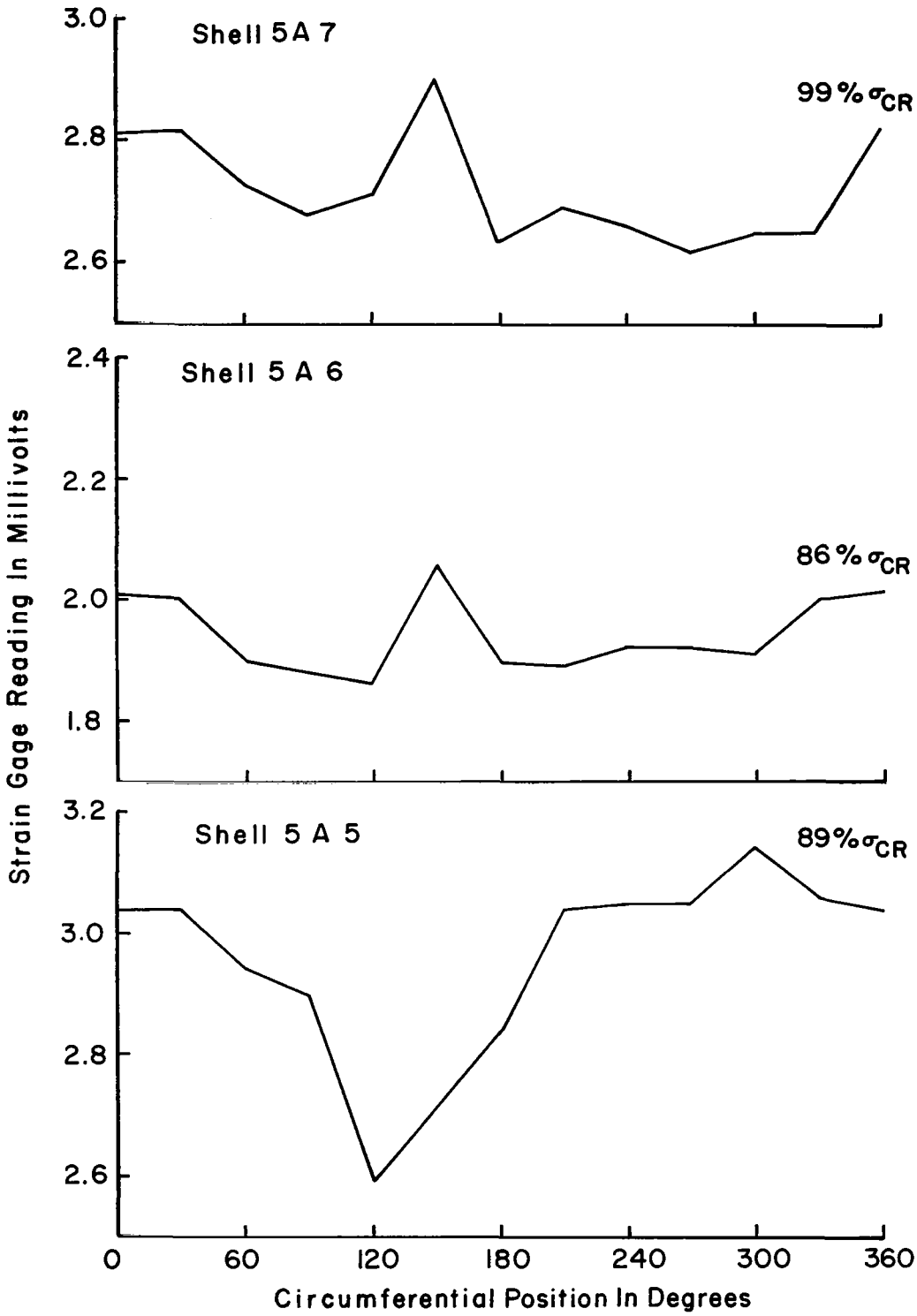

FIG. 18 LOAD DISTRIBUTION NEAR BUCKLING (SHELLS 5A5, 5A6, 5A7)

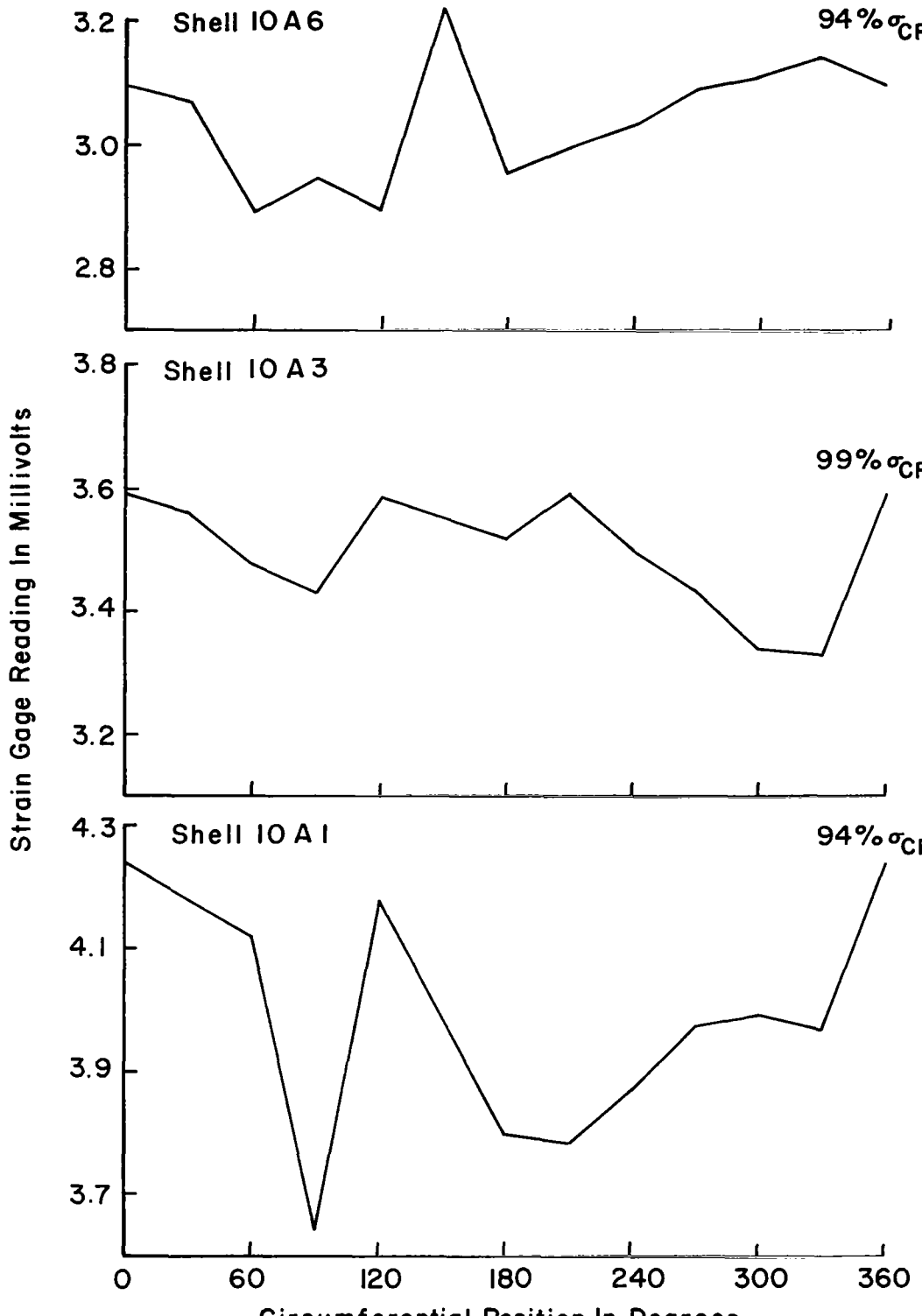

FIG. 19 LOAD DISTRIBUTION NEAR BUCKLING (SHELLS 10A1, 10A3, 10A6)

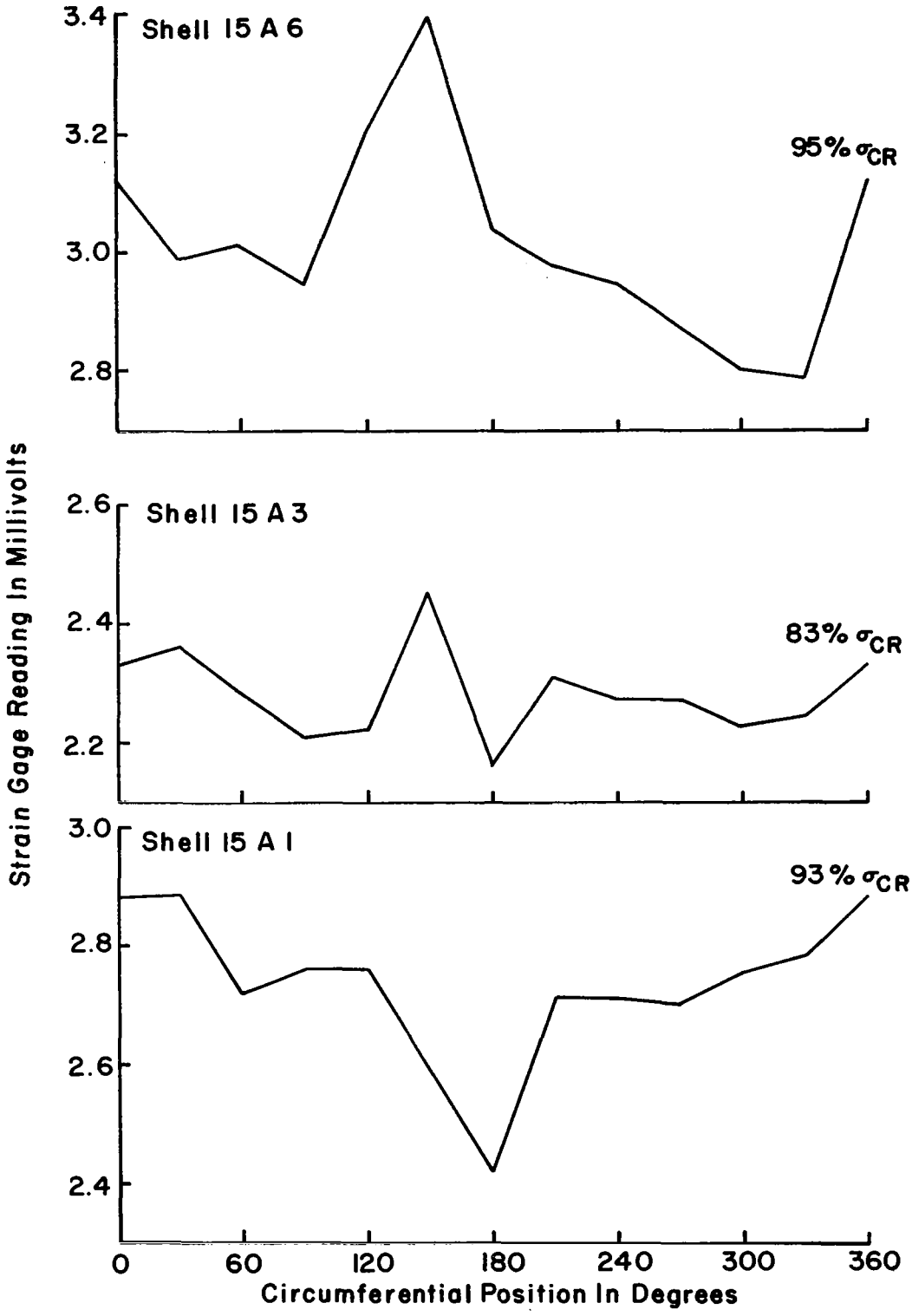

FIG. 20 LOAD DISTRIBUTION NEAR BUCKLING (SHELLS 15A1, 15A3, 15A6)

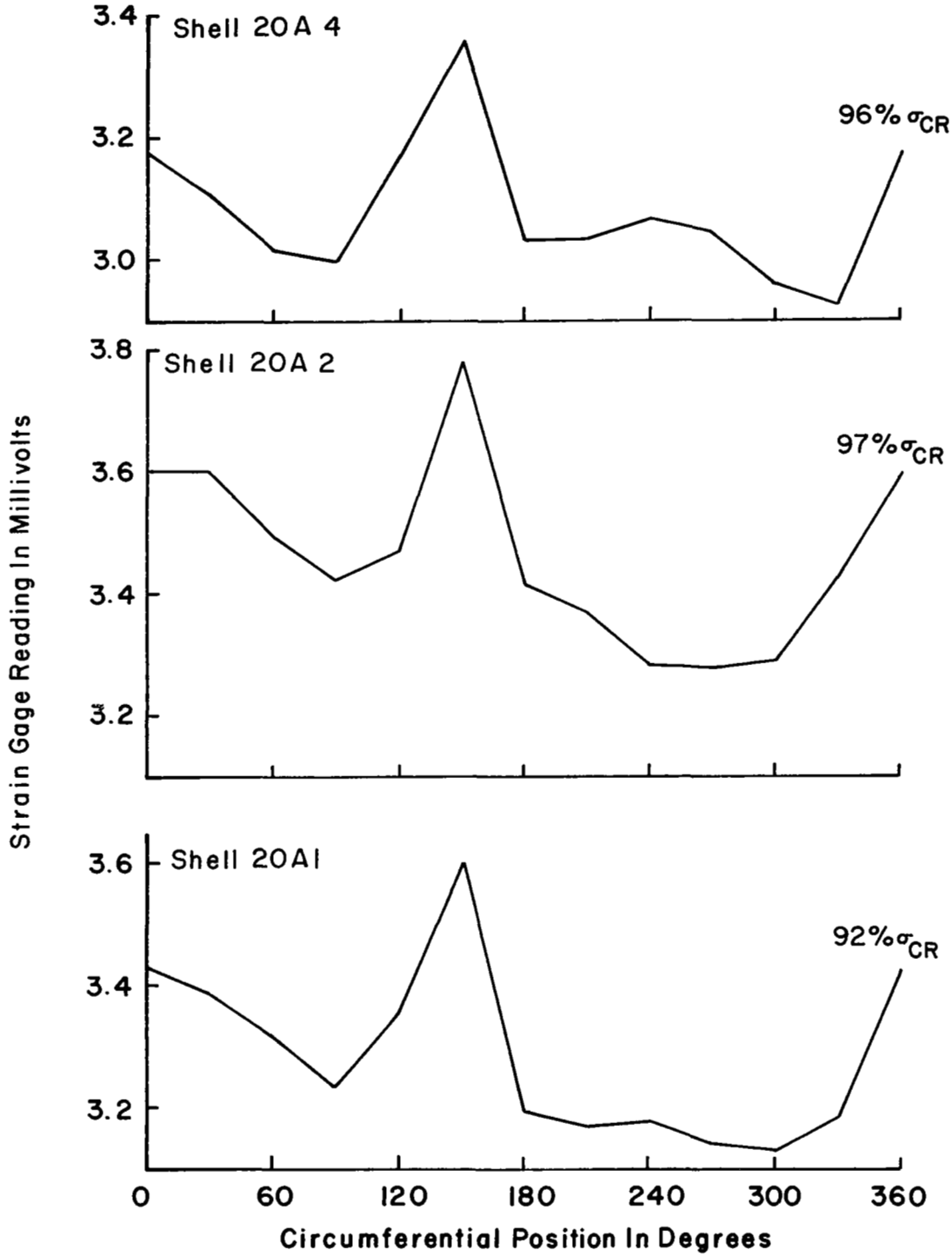

FIG. 21 LOAD DISTRIBUTION NEAR BUCKLING (SHELLS 20A1, 20A2, 20A4)

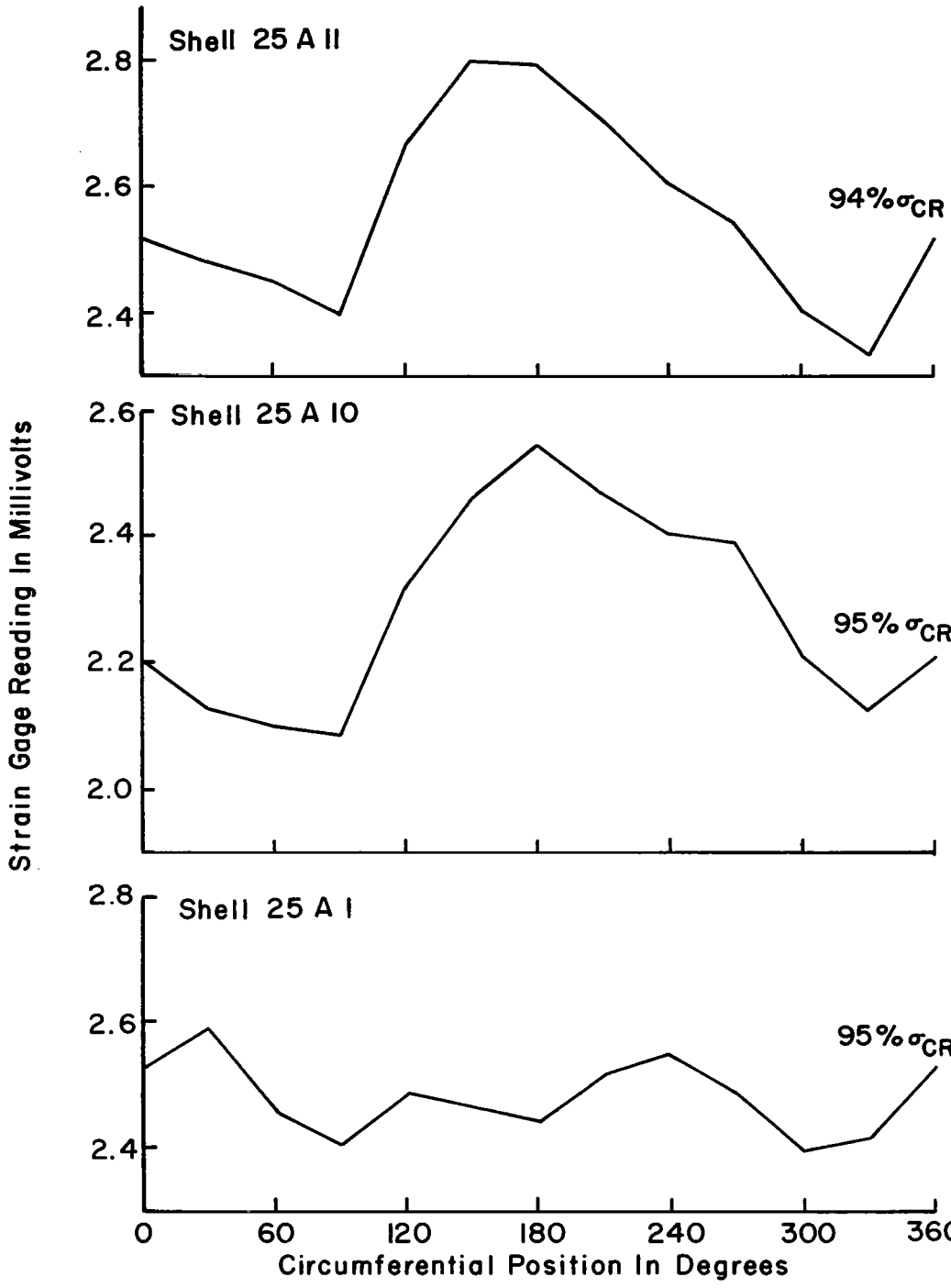

FIG. 22 LOAD DISTRIBUTION NEAR BUCKLING (SHELLS 25 A I, 25 A 10, 25A II)

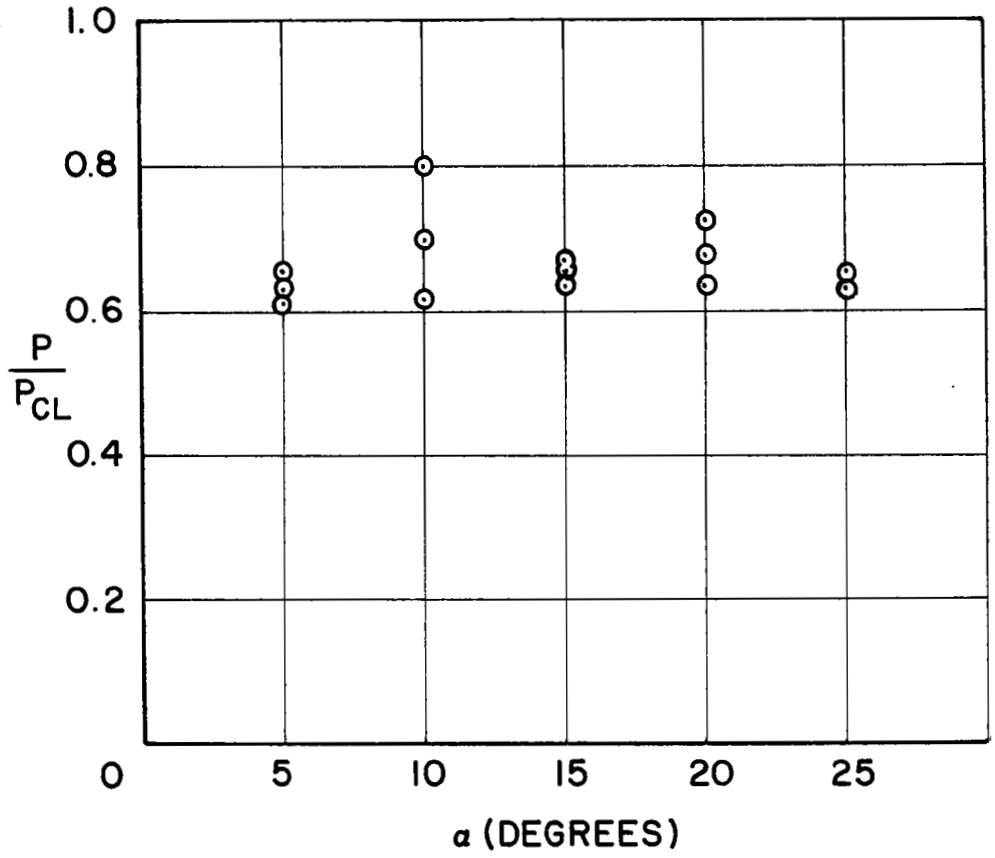

FIG. 23 AXIAL BUCKLING LOAD VS CONE ANGLE FOR "PERFECT" CONICAL SHELLS

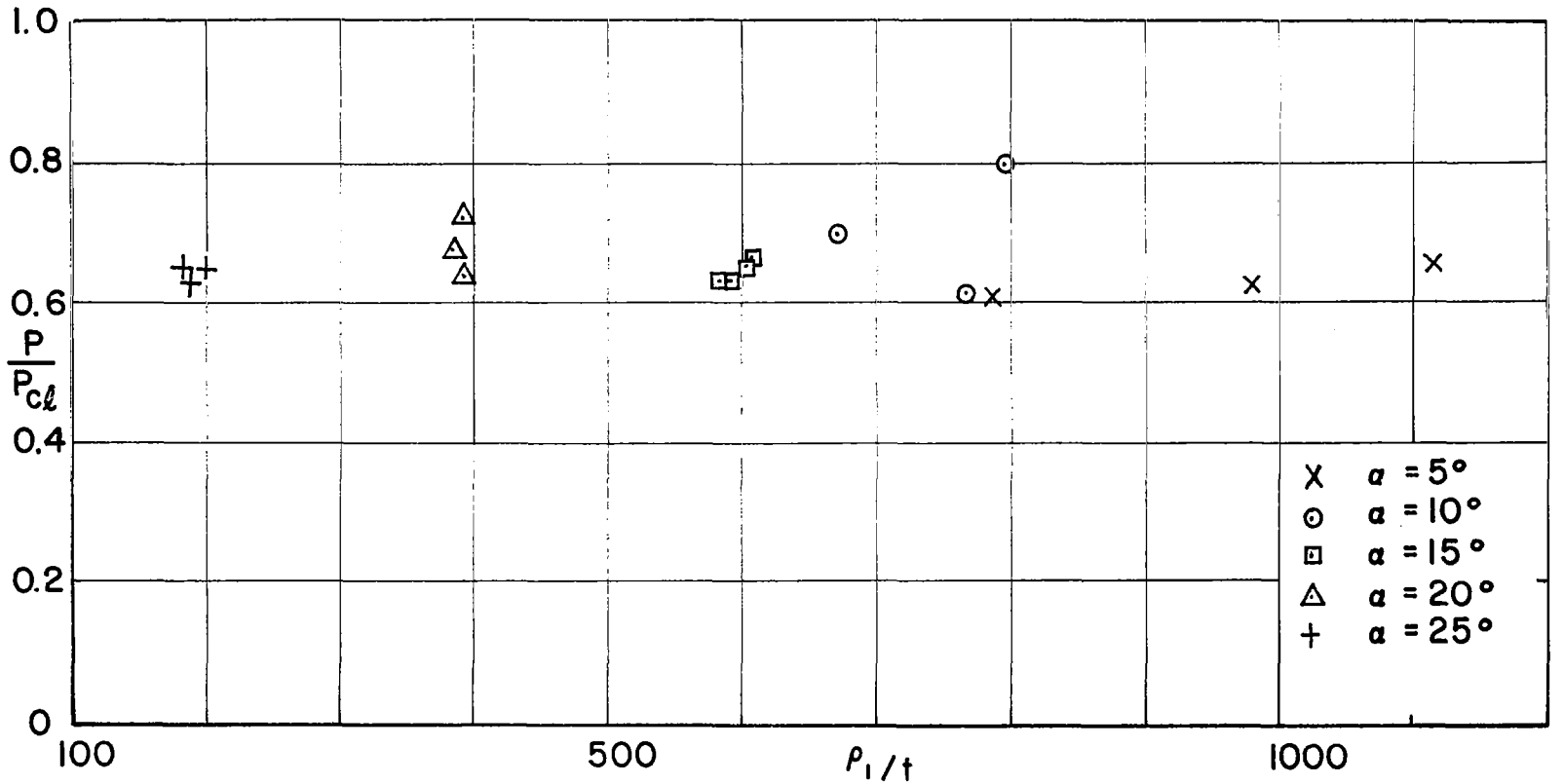

FIG. 24 AXIAL BUCKLING LOAD VS RADIUS OF CURVATURE AT THE SMALL END OVER THICKNESS RATIO FOR "PERFECT" CONICAL SHELLS

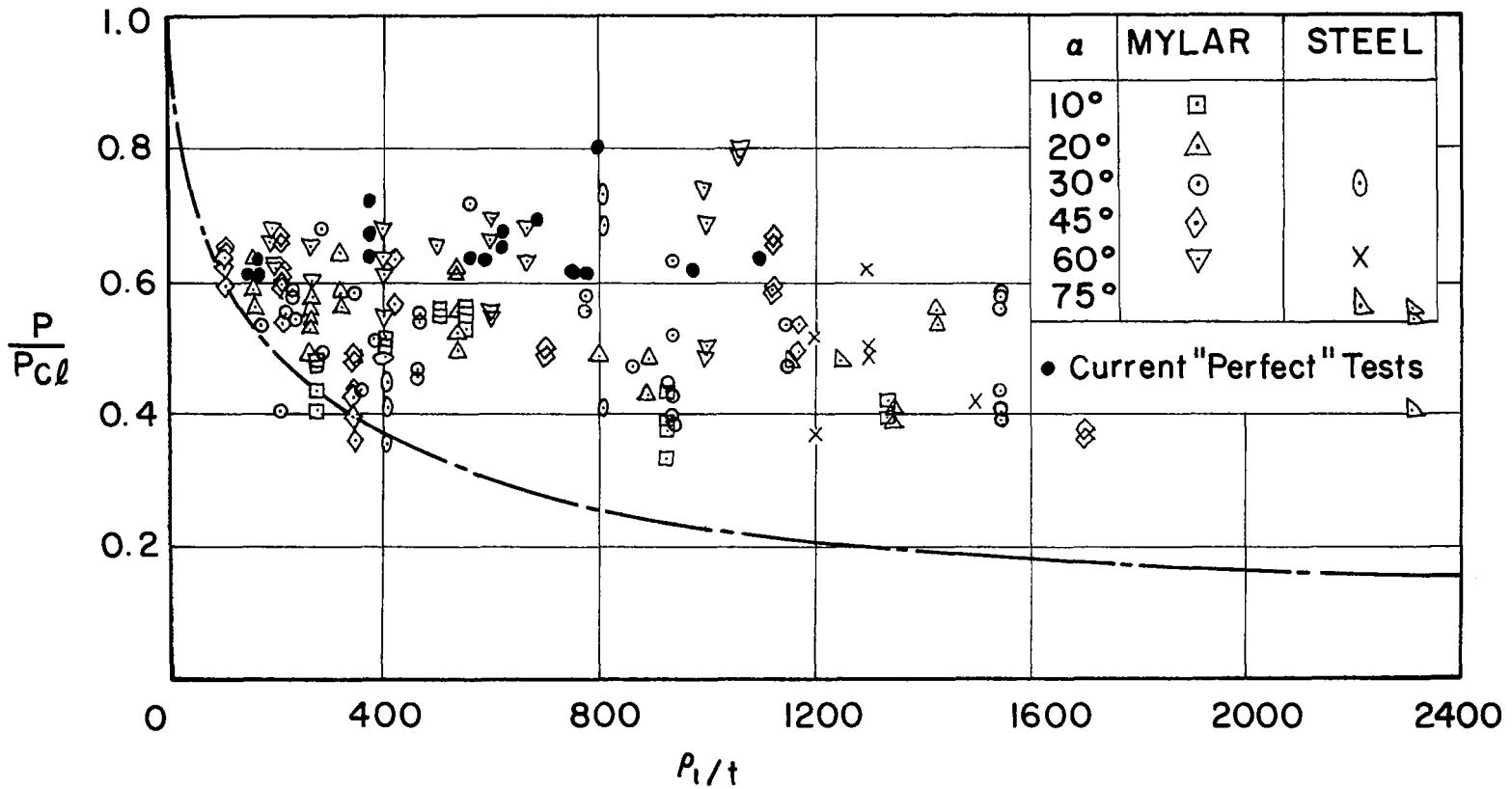

FIG.25 COMPARISON OF AXIAL BUCKLING LOAD OF CONICAL SHELLS WITH LOWER BOUND CURVE FOR CYLINDERS

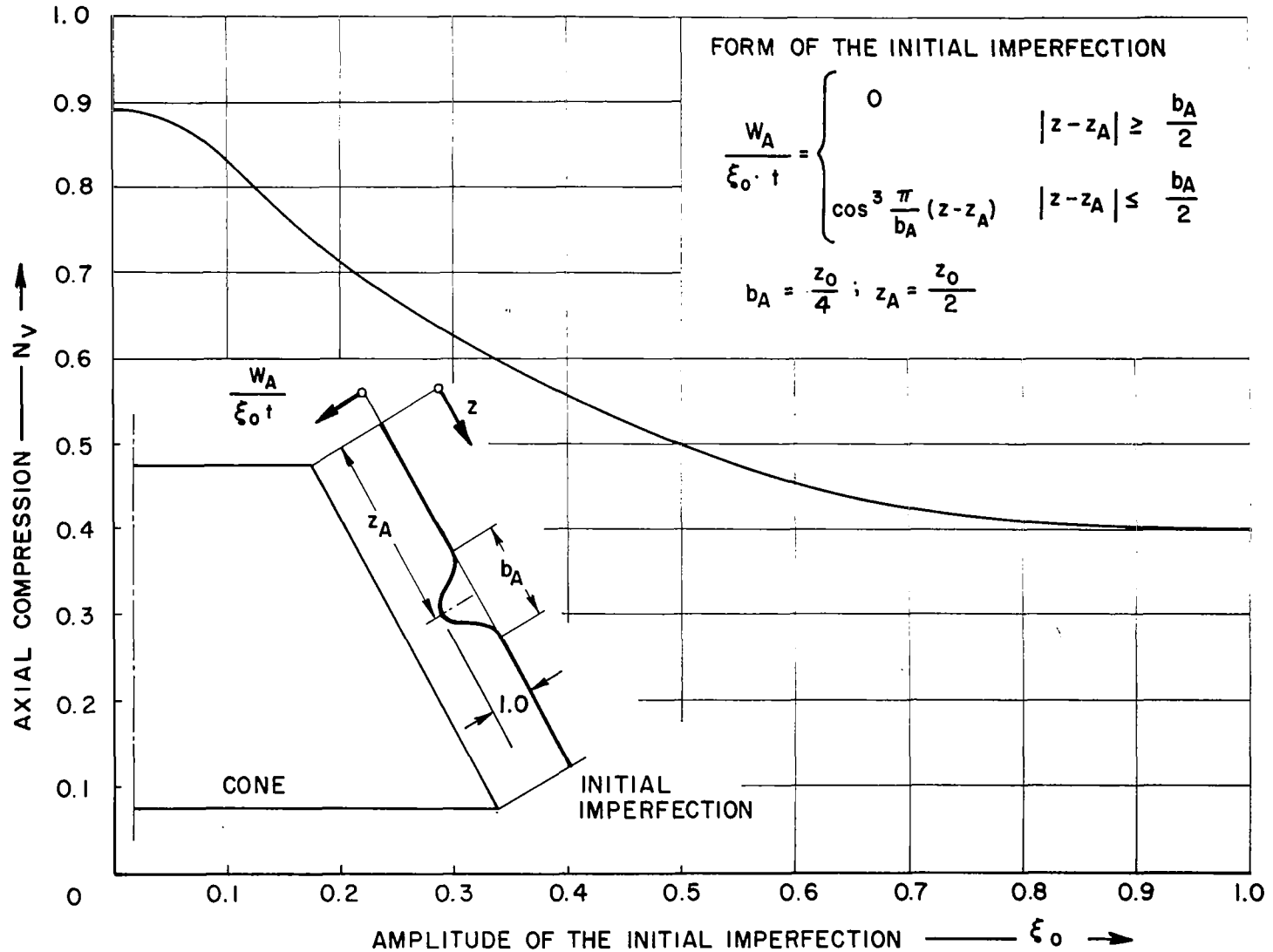

FIG.26 AMPLITUDE OF THE INITIAL IMPERFECTION VS BUCKLING LOAD

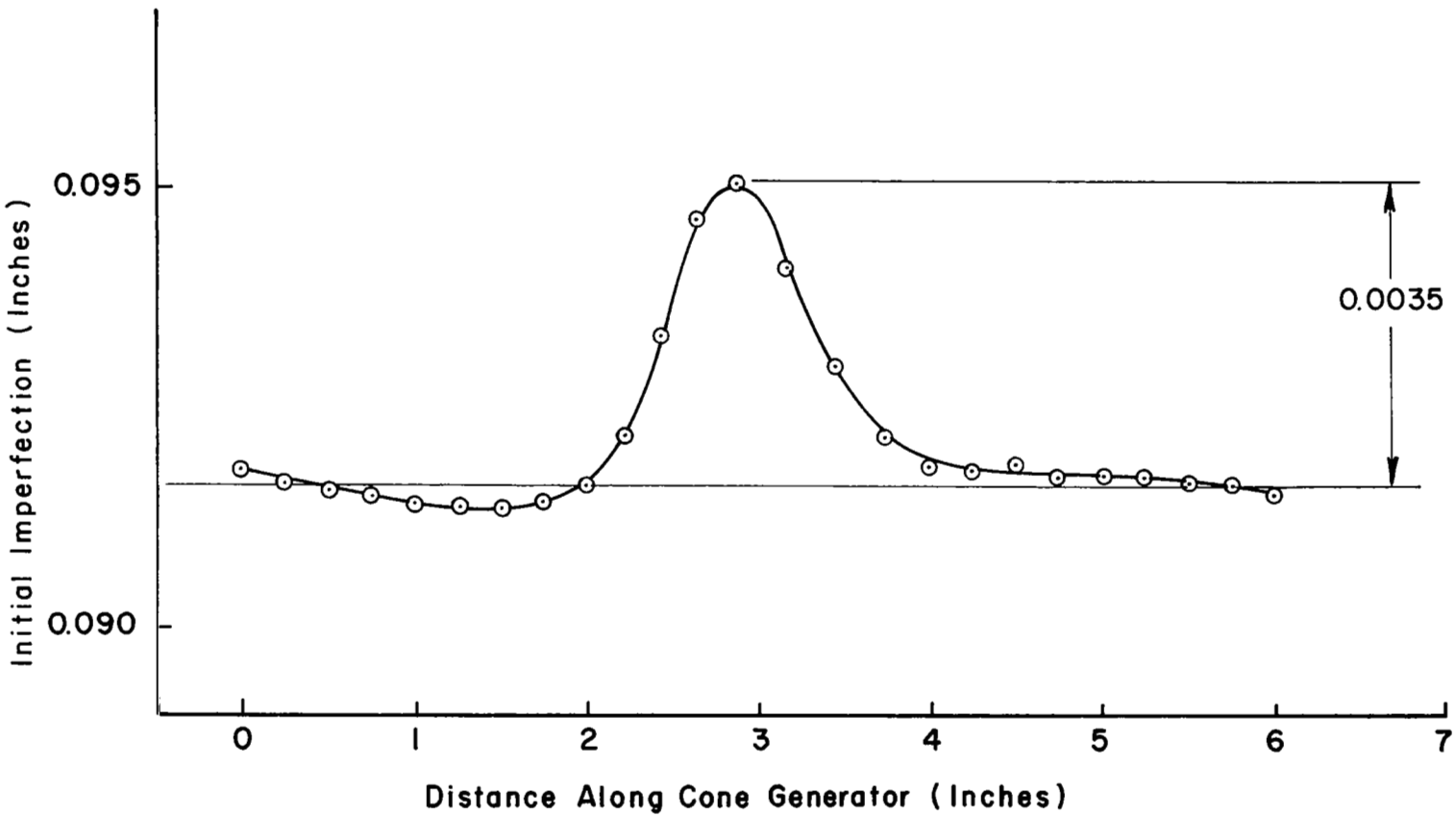

FIG. 27 SHELL 2011 INITIAL IMPERFECTION

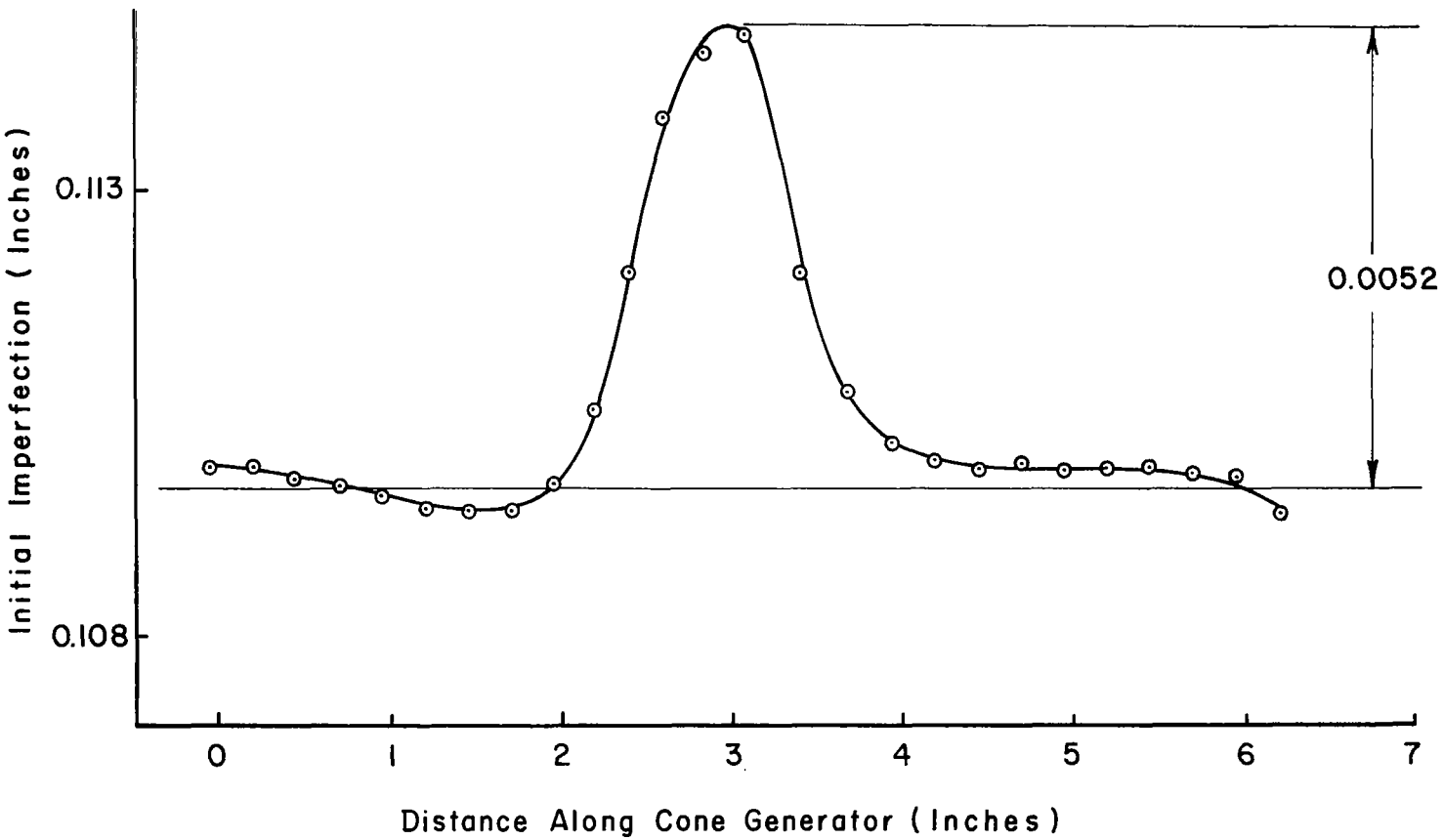

FIG. 28 SHELL 2012 INITIAL IMPERFECTION

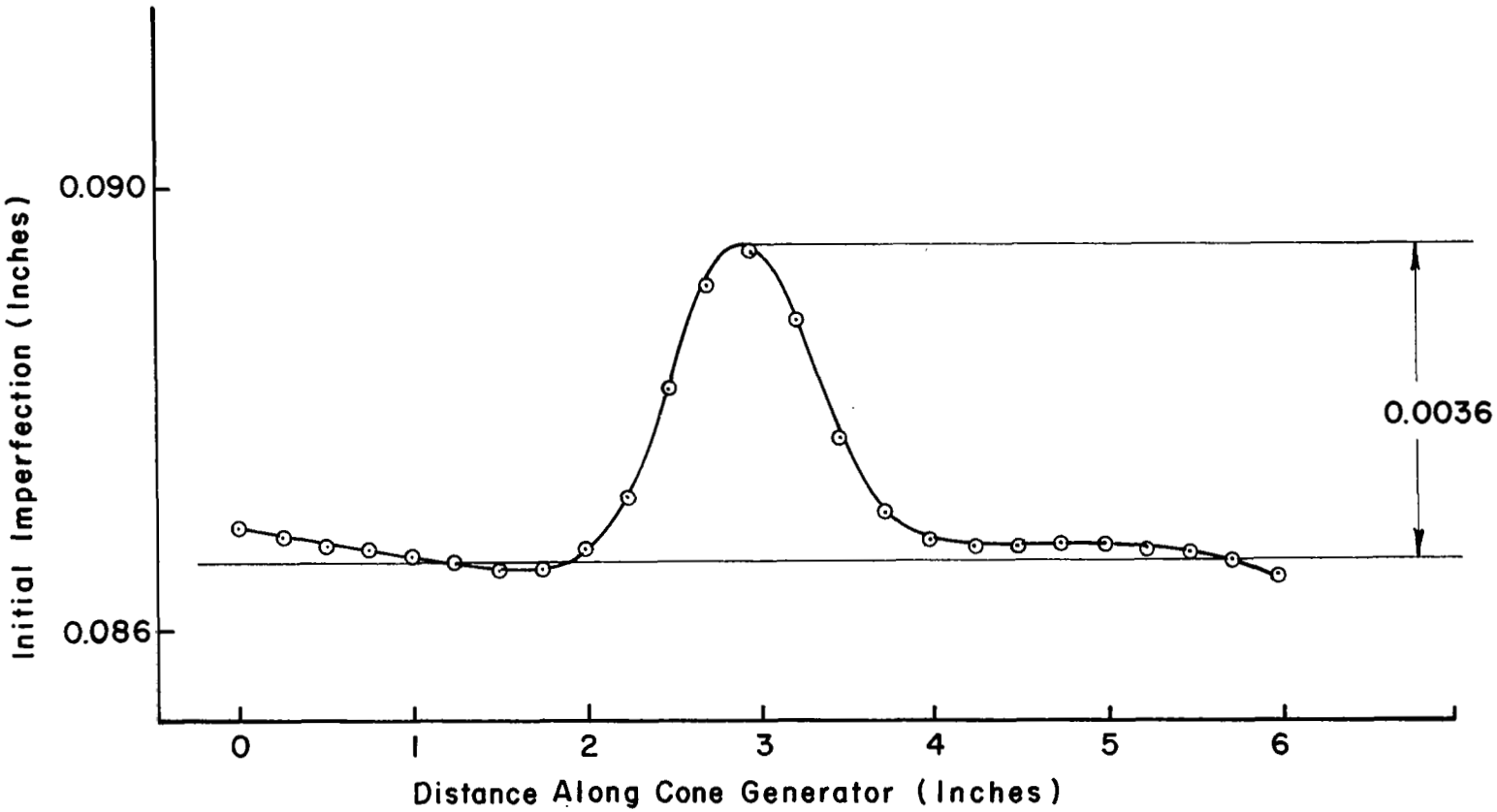

FIG. 29 SHELL 2013 INITIAL IMPERFECTION

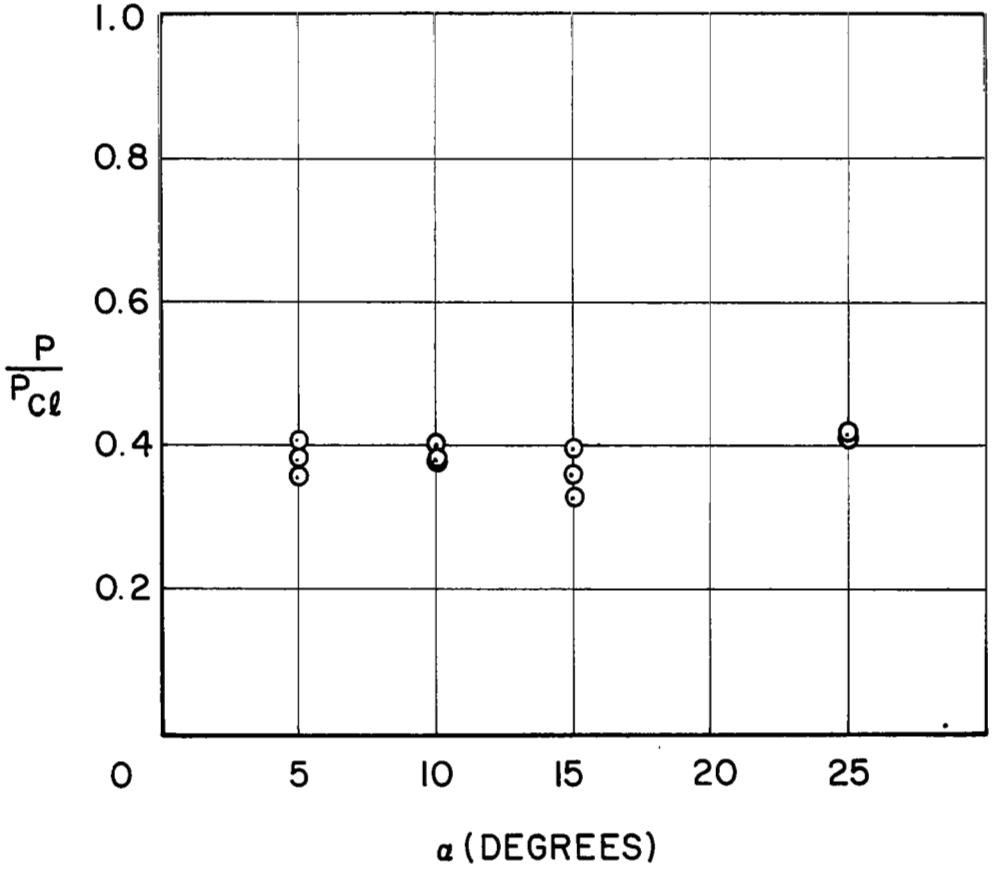

FIG.30 AXIAL BUCKLING LOAD VS CONE ANGLE FOR "IMPERFECT" CONICAL SHELLS

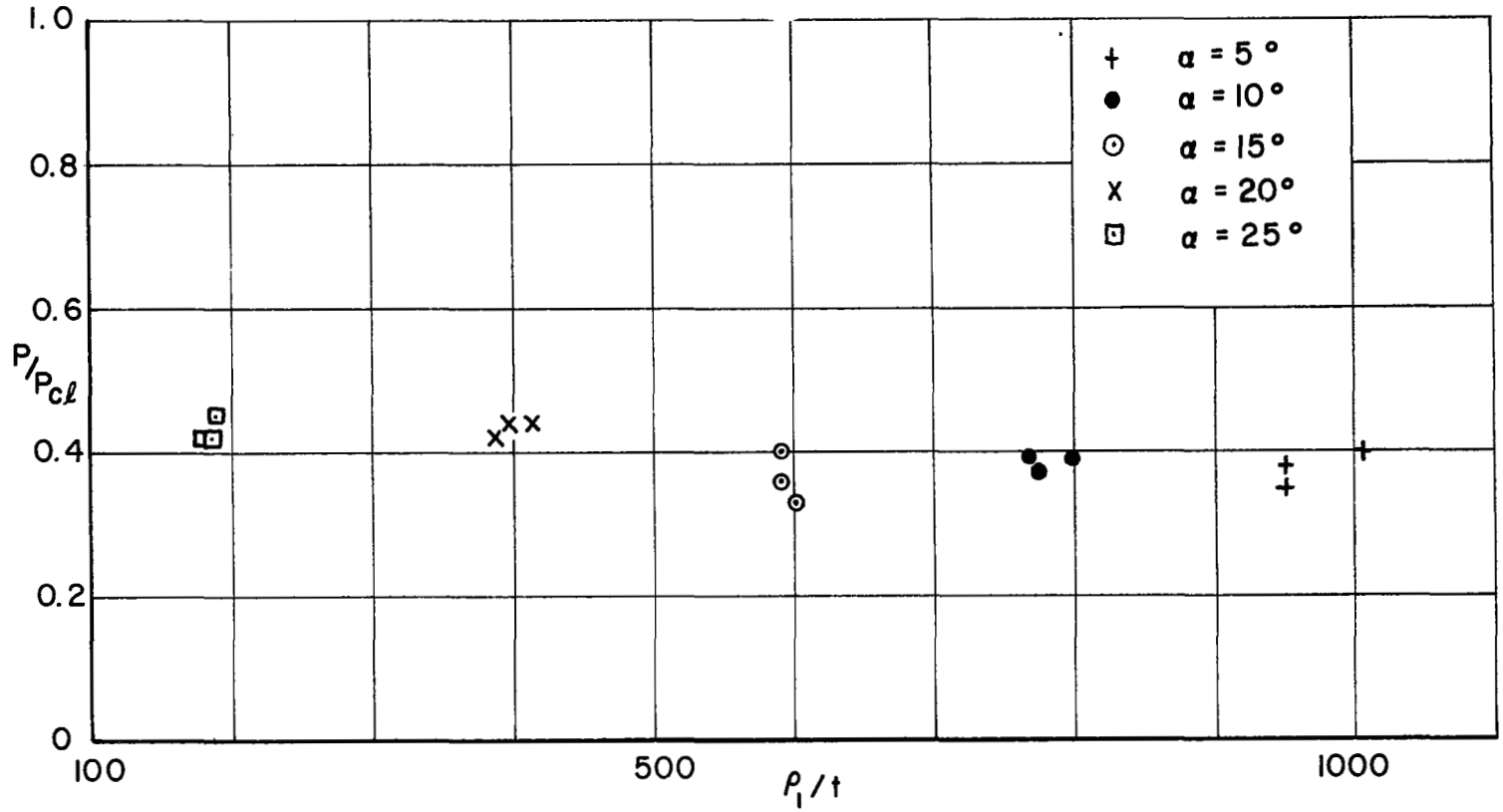

FIG. 31 AXIAL BUCKLING LOAD VS. RADIUS OF CURVATURE AT THE SMALL END OVER THICKNESS RATIO FOR "IMPERFECT" CONICAL SHELLS

NASA-Langley, 1968 — 32 CR-1162